J|A|C|S
ARTICLES
Published on Web 10/03/2006

A Conformational Study of Phospha(III)- and Phospha(V)-guanidine Compounds

Natalie E. Mansfield, Joanna Grundy, Martyn P. Coles,* Anthony G. Avent, and Peter B. Hitchcock

Contribution from the Department of Chemistry, University of Sussex, Falmer, Brighton BN1 9QJ, UK

Received June 15, 2006; E-mail: m.p.coles@sussex.ac.uk

Abstract: Spectroscopic, crystallographic, and computational studies of the substituent distribution about the "NCN" unit in a series of phospha(III)- and phospha(V)-guanidines, $R_2PC\{NR'\}\{NHR'\}$ and $R_2P(E)C\{NR'\}\{NHR'\}$ (R = Ph, Cy; R′ = ^{i}Pr, Cy; E = S, Se), are reported. In the phosphorus(III) systems, the *P*-diphenyl substituted compounds are observed as only one isomer, shown by NMR spectroscopy to be the E_{syn}-(α) configuration. In contrast, the corresponding *P*-dicyclohexyl derivatives exist as a mixture of E_{syn}-(α) and Z_{anti} in solution. Spectroscopic techniques are unable to determine whether the latter isomer exists as the α- or β-conformer relative to rotation about the P−$C_{amidine}$ bond; however, DFT calculations indicate a low-energy structure for the *N,N*′-dimethyl model complex in the β-conformation. In their oxidized sulfo and seleno forms, the *P*-diphenyl compounds are present as an interconverting equilibrium mixture of the E_{syn}-(β) and Z_{syn}-(β) isomers in solution (~3:2 ratio), whereas for the *P*-dicyclohexyl analogues, the latter configuration (in which the nitrogen substituents are in a more sterically unfavorably *cisoid* arrangement about the imine double bond) is the dominant form. Intramolecular E···HN (E = S, Se) interactions are observed in solution for the Z_{syn}-(β) configuration of both *P*-substituted species, characterized by J_{SeH} coupling in the NMR spectrum for the P(V)-seleno compounds and a bathochromic shift of the N*H* absorption in the infrared spectrum. An X-ray crystallographic analysis of representative $Ph_2P(E)$- and $Cy_2P(E)$-substituted species shows exclusively the E_{syn}-(β) configuration for the *P*-diphenyl substituted compounds and the Z_{syn}-(β) form for the *P*-dicyclohexyl derivatives, independent of the chalcogen and the nitrogen substituents. Results from a DFT analysis of model compounds fail to identify a compelling electronic argument for the observed preferences in substituent orientation, suggesting that steric factors play an important role in determining the subtle energetic differences at work in these systems.

Introduction

Amidines and guanidines comprise two closely related families of organic molecules with general formula $R^{(1)}C\{NR^{(2)}\}\{NR^{(3)}R^{(4)}\}$ (amidine: $R^{(1)}$ = hydrogen, alkyl, aryl; guanidine: $R^{(1)}$ = amido; $R^{(2)-(4)}$ = hydrogen, alkyl, aryl, silyl) which, by virtue of their multiple functionality and high level of substituent tunability, have attained prominence in a number of different fields of chemistry. Much of the drive to develop new substitution patterns around the amidine and guanidine frameworks derives from their widespread application as ligands in coordination chemistry.[1] In this context, significant work has focused on the tri- and tetra-substituted amidine and guanidine compounds, respectively (i.e., $R^{(4)}$ = H), where retention of a single N*H* functionality facilitates conversion to the corresponding amidinate and guanidinate anions, which readily coordinate to metals from throughout the periodic table.[2]

One of the often overlooked yet fundamental features associated with both classes of neutral compounds is the ability of the nitrogen substituents, $R^{(2)-(4)}$, to adopt different isomeric arrangements and, when a hydrogen substituent is present, tautomeric arrangements about the ligand framework (Figure 1).[3] As current interest is moving toward the application of these families of compounds as reagents in asymmetric systems (e.g., organocatalysis,[4] anion recognition[5]), factors which determine the relative stability of these different conformers are likely to play increasingly important contributions in the intelligent design of new reagents during the development of these areas.

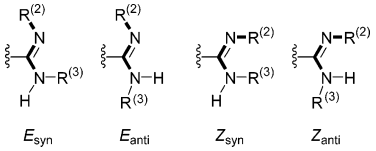

Figure 1. The four configurations of *N*-substituents within a trisubstituted amidine unit.

As part of our continued interest in the coordination chemistry of neutral amidines and guanidines,[6,7] we have incorporated additional phosphorus-based functionality within the general

(1) Coles, M. P. *Dalton Trans.* **2006**, 985.
(2) Barker, J.; Kilner, M. *Coord. Chem. Rev.* **1994**, *133*, 219−300; Edelmann, F. T. *Coord. Chem. Rev.* **1994**, *137*, 403; Bailey, P. J.; Pace, S. *Coord. Chem. Rev.* **2001**, *214*, 91.
(3) Häfelinger, G.; Kuske, F. K. H. In *The Chemistry of Amidines and Imidates*; Patai, S., Rappoport, Z., Eds. Wiley: Chichester, 1991; Vol. 2.
(4) Köhn, U.; Günther, W.; Görls, H.; Anders, E. *Tetrahedron: Asymmetry* **2004**, *15*, 1419.
(5) Schug, K. A.; Lindner, W. *Chem. Rev.* **2005**, *105*, 67.

Scheme 1. Synthetic Procedures Employed during This Study (**a**, R′ = ^{i}Pr; **b**, R′ = Cy; { } Denotes Previously Reported Compounds That Are Included in This Report for Comparative Purposes)[a]

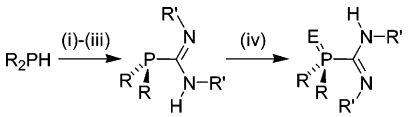

{**1a**,**b**} R = Ph {**3a**,**b**} R = Ph, E = S
2a,**b** R = Cy {**4a**,**b**} R = Ph, E = Se
5a,**b** R = Cy, E = S
6a,**b** R = Cy, E = Se

[a] Reagents and conditions: (i) ^{n}BuLi, THF, −78 °C; (ii) R′N=C=NR′, THF, 0 °C; (iii) [HNEt$_3$][Cl], THF, 25 °C; (iv) elemental E (E = S, Se), toluene, 25 °C

amidine framework at the central carbon position. A series of compounds with general formula $R_2PC\{NR'\}\{NHR'\}$ have been prepared,[8,9] which are referred to as phospha(III)guanidines by analogy to their nitrogen-substituted guanidine relatives, $R_2NC\{NR'\}\{NHR'\}$ (Scheme 1). We have recently extended this work to prepare di(phospha(III)guanidine) compounds that have been used in the formation of bimetallic species and have been shown to function as a chelating diphosphine-type ligand at late transition metals.[10]

Conversion of the phosphaguanidines to the corresponding P(V)-chalcogeno analogues has been achieved in a straightforward manner by employing elemental sulfur and selenium to give the corresponding sulfo- and selenophospha(V)guanidines (Scheme 1).[11] During studies of the oxidized species {**3a**,**b**} and {**4a**,**b**}, variation in the geometric arrangement of the nitrogen substituents in solution was noted. It was established, using multinuclear NMR spectroscopy, that at room temperature two interchanging species were present that corresponded to an equilibrium mixture of the E_{syn} and Z_{syn} configurational isomers. This observation was rationalized in terms of the formation of an attractive, "nonbonded" interaction between the chalcogen and the amino N*H*, locking the amidine in position by restricting rotation about the P−C bond. As a result, steric conflict between the imine and phosphorus substituents becomes a major factor in determining the relative stability of the different configurations, causing the C=N double bond to isomerize to relieve unfavorable interactions. Consideration of the electronic contribution to this rearrangement was not probed in detail, although reference was made to the zwitterionic nature of the phosphorus−chalcogen bond facilitating formation of the N*H*···E=P interaction.

A convenient parameter that may be used to compare the (non)planarity of three-coordinate atoms is the degree of pyramidalization DP(%),[12] defined as:

$$\mathrm{DP}(\%) = \frac{[360 - \sum_{i=1}^{3}\alpha]}{0.9}$$

where the sum covers the three smallest bond angles, α_i, of the atom under consideration. The resultant value gives an estimation of the deviation of the three bond angles from the full angle (normalized to 90°) ranging from 0% (planar) to 100% for maximum pyramidalization, achieved when the sum of the three angles is equal to 270°, corresponding to three mutually perpendicular $2p_N$ atomic orbitals. Examples of structurally characterized guanidines in which the tertiary amino substituents do not form part of a heterocycle (thus imposing steric restrictions on the displacement of these groups) are rare.[13] The bond parameters for these compounds, in addition to examples in which the guanidine is coordinated to a metal center,[7,14] all indicate a strong tendency for the formation of planar tertiary amino nitrogen atoms [DP values in the range 0−7.9%], consistent with significant delocalization of electron density into the "NCN" component of the molecule. The equivalent overlap between the phosphorus lone pair and the sp^2-carbon in phospha(III)guanidines is energetically unfavorable, resulting in a pyramidal arrangement of *P*-substituents as noted in the solid-state structures of {**1a**} [DP = 62.7%] and {**1b**} [DP = 60.1%]. When considered alongside the localized carbon−nitrogen bonding within the "NCN" unit, which renders the nitrogen groups inequivalent, this pyramidal geometry introduces the possibility of conformational isomers within the phosphaguanidine compounds, denoted α and β in this work (Scheme 2). The occupation of the fourth vertex of the pyramidal phosphorus by the chalcogen atom in the P(V) derivatives {**3a**,**b**} and {**4a**,**b**} leads to the same geometrical considerations when discussing these systems.

Scheme 2. Schematic Description of the (α) and (β) Conformers in Phospha(III)guanidines (X = Lone Pair, Chalcogen)

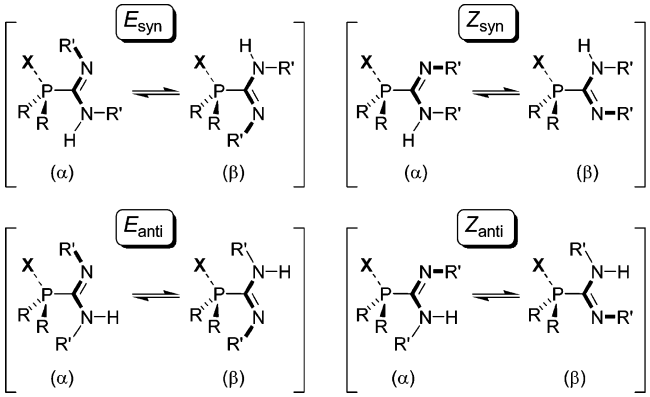

To be distinguishable from each other using standard analytical techniques, certain limitations regarding fluxional processes need to be met: (a) restricted (or slow) rotation about the R_2P-CN_2 bond; (b) a high barrier to inversion for phosphorus in the P(III) derivatives; (c) a slow rate of hydrogen exchange between the different nitrogen atoms, particularly relevant in the case of the E_{anti} configuration. The energetics of interchange between these forms will be influenced by not only the steric

(6) Oakley, S. H.; Coles, M. P.; Hitchcock, P. B. *Inorg. Chem.* **2003**, *42*, 3154; Oakley, S. H.; Coles, M. P.; Hitchcock, P. B. *Inorg. Chem.* **2004**, *43*, 5168; Oakley, S. H.; Soria, D. B.; Coles, M. P.; Hitchcock, P. B. *Polyhedron* **2006**, *25*, 1247.
(7) Oakley, S. H.; Soria, D. B.; Coles, M. P.; Hitchcock, P. B. *Dalton Trans.* **2004**, 537.
(8) Coles, M. P.; Hitchcock, P. B. *Chem. Commun.* **2002**, 2794.
(9) Grundy, J.; Coles, M. P.; Hitchcock, P. B. *Dalton Trans.* **2003**, 2573.
(10) Mansfield, N. E.; Coles, M. P.; Avent, A. G.; Hitchcock, P. B. *Organometallics* **2006**, 2470.
(11) Grundy, J.; Coles, M. P.; Avent, A. G.; Hitchcock, P. B. *Chem. Commun.* **2004**, 2410.
(12) Maksiæ, Z. B.; Kovaèevic, B. *J. Chem. Soc., Perkin Trans. 2* **1999**, 2623.
(13) Heinisch, G.; Matuszczak, B.; Rakowitz, D.; Mereiter, K. *J. Heterocycl. Chem.* **2002**, *39*, 695; Ghosh, R.; Samuelson, A. G. *Chem. Commun.* **2005**, 2017.
(14) Birch, S. J.; Boss, S. R.; Cole, S. C.; Coles, M. P.; Haigh, R.; Hitchcock, P. B.; Wheatley, A. E. H. *Dalton Trans.* **2004**, 3568; Coles, M. P.; Hitchcock, P. B. *Eur. J. Inorg. Chem.* **2004**, 2662.

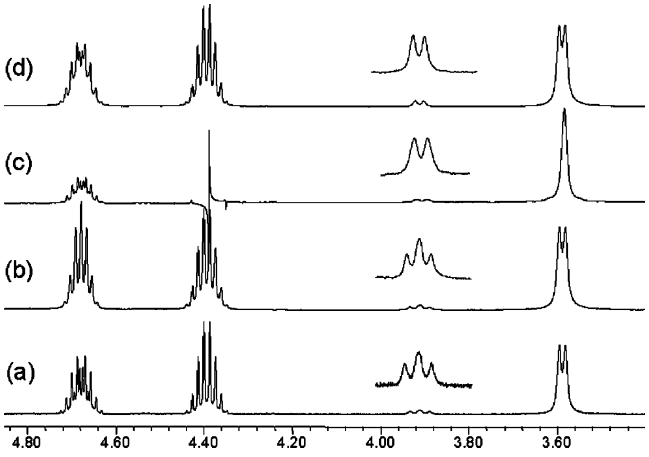

Figure 2. Results from selective decoupling experiments in ^{1}H NMR spectroscopy for **2a**, showing the isopropyl methine resonances of the major isomer, and N*H* resonances for both species present in solution: (a) full spectrum; (b) major phosphorus resonance decoupled; (c) N_{amine} methine resonance decoupled; (d) minor phosphorus resonance decoupled.

properties of the substituents, but also the N*H*···E═P nonbonded interactions previously noted in the phospha(V)guanidine system.

This paper describes the previously unreported *P*-dicyclohexyl derivatives of the P(III)- and P(V)phosphaguanidines, enabling detailed structural comparisons to be made with the *P*-diphenyl compounds. The results from a combined spectroscopic and crystallographic study have enabled further understanding of the key features that influence the configurational preferences to be established. In addition, DFT studies have been conducted to probe the electronic factors involved in determining the relative stabilities of different arrangements of substituents.

Results and Discussion

Synthesis and Spectroscopic Analysis of Phospha(III)-guanidines, $R_2PC\{NR'\}\{NHR'\}$. The general synthetic methodology that we have employed in the synthesis of *P*-diphenylphospha(III)guanidines,[9] has been extended to encompass the corresponding *P*-dicyclohexyl analogues, $Cy_2PC\{NR'\}\{NHR'\}$ [**2a**, R′ = ^{i}Pr; **2b**, R′ = Cy, Scheme 1]. The neutral compounds were isolated as white, crystalline solids in high yield (75−80%) by crystallization from concentrated hexane at −30 °C. In contrast to the *P*-diphenyl analogues {**1a**,**b**}, multinuclear NMR analysis of analytically pure samples indicated the presence two isomers in solution, most evident from $^{31}P\{^1H\}$ NMR data [**2a** (14:1 ratio), δ_{major} −21.2; δ_{minor} −4.8. **2b** (12:1 ratio), δ_{major} −21.1; δ_{minor} −4.1]. The N^{i}Pr substituted compound, **2a**, was selected for a detailed NMR spectroscopic analysis due to the simplified spectra in comparison to the *per*-cyclohexyl derivative, **2b**; comparable solution-state behavior is, however, observed for each compound and it is therefore reasonable to assume similar fluxional processes operating for both compounds.

The room temperature ^{1}H NMR spectrum of **2a** indicates that each isomeric form has inequivalent nitrogen substituents, consistent with localized C═N double and C−N single bonds within the amidine unit [(a), Figure 2]. The septet corresponding to the N_{imine} methine proton of the major isomer at δ 4.68 exhibits additional coupling to phosphorus, demonstrated by simplification of this multiplet upon selective decoupling of the corresponding phosphorus resonance at δ −21.2 (Figure 2b). Selective decoupling of the other septet at 4.39 ppm, corresponding to the N_{amine} methine of the major species, results in the collapse of the N*H* resonance at δ 3.59 to a single broad resonance (Figure 2c), indicating the origin of this doublet is a $^3J_{HH}$ coupling rather than coupling to phosphorus. It was also observed during this experiment that the N*H* signal of the minor component, present as a pseudotriplet corresponding to an unresolved doublet of doublets at δ 3.91, collapsed to a doublet indicating the N_{amine} methine resonance of the minor species is coincident with the septet at 4.39 ppm. The additional component that contributes to the splitting of the N*H* resonance was shown to be a $^3J_{HP}$ coupling of similar magnitude, demonstrated by decoupling the minor phosphorus resonance at δ −4.8 (Figure 2d).

A large, positive nOe between the amino proton and the *P*-cyclohexyl substituents in the major isomer is consistent with the E_{syn}-(α) configuration predominating in solution. Similar experiments indicate an interaction between the N*H* and the N_{imine} isopropyl group in the minor isomer, suggesting a Z_{anti} arrangement of substituents, although assignment to the specific α- or β-conformation form is not possible solely on the basis of these data. These observations differ to those made for the *P*-diphenyl compounds {**1a**,**b**}, where only the E_{syn}-(α) is observed in solution over the temperature range 298−333 K, giving the first indication that, despite being remote from one another, the phosphorus substituents exert an influence on the relative energies of the different configurations of the amidine unit.

Irradiation of the N_{imine} methine resonance of **2a** induces a large negative nOe of the corresponding methine resonance of the N_{amine} substituent, signifying an exchange process between these two groups. Since the barrier to inversion at phosphorus is a relatively high-energy process (typically in the range 35−38 kcal mol^{-1}),[15] a mechanism by which this is occurring is proposed involving a hydrogen exchange between the two *N*-atoms. While it is possible that an *inter*molecular process may be taking place involving two (or more) molecules of **2a**, no concentration dependence was observed for this interconversion, suggesting an intramolecular process. The corresponding hydrogen-exchange process in *P*-diphenyl derivative {**1a**} is only observed upon heating the sample to 333 K, consistent with a higher-energy process. Variable-temperature NMR spectroscopy performed on **2a** shows a change in the ratio of 14:1 noted at 298 K to 9:1 at 343 K. Van't Hoff analysis of the data gave a value for ΔH of 1.9 kcal mol^{-1}, with the corresponding entropy value of +1.2 eu. Interpretation of these data is, however, complicated by the existence of greater than one fluxional process taking place within these compounds (vide infra).

Scheme 3 summarizes proposed mechanisms for the fluxional processes observed for **2a** in solution. In Pathway 1 {proton exchange}, rotation of the C−N single bond initially converts the E_{syn}-(α) form to the E_{anti}-(α), followed by proton transfer between the two nitrogen atoms. This mechanism is reasonable, considering steric terms, as it has been shown that the anions of **2a**,**b** are able to adopt an *N*,*N*′-chelating coordination mode

(15) Lehn, J. M.; Munsch, B. *J. Chem. Soc., Chem. Commun.* **1969**, 1327; Baechler, R. D.; Farnham, W. B.; Mislow, K. *J. Am. Chem. Soc.* **1969**, *91*, 5686; Baechler, R. D.; Mislow, K. *J. Am. Chem. Soc.* **1970**, *92*, 3090; Mislow, K.; Baechler, R. D. *J. Am. Chem. Soc.* **1971**, *93*, 773; Fryzuk, M. D.; Giesbrecht, G. R.; Rettig, S. J. *Inorg. Chem.* **1998**, *37*, 6928.

Scheme 3. Possible Mechanisms Allowing Interconversion of the Different Isomeric Forms of Phospha(III)guanidines in Solution

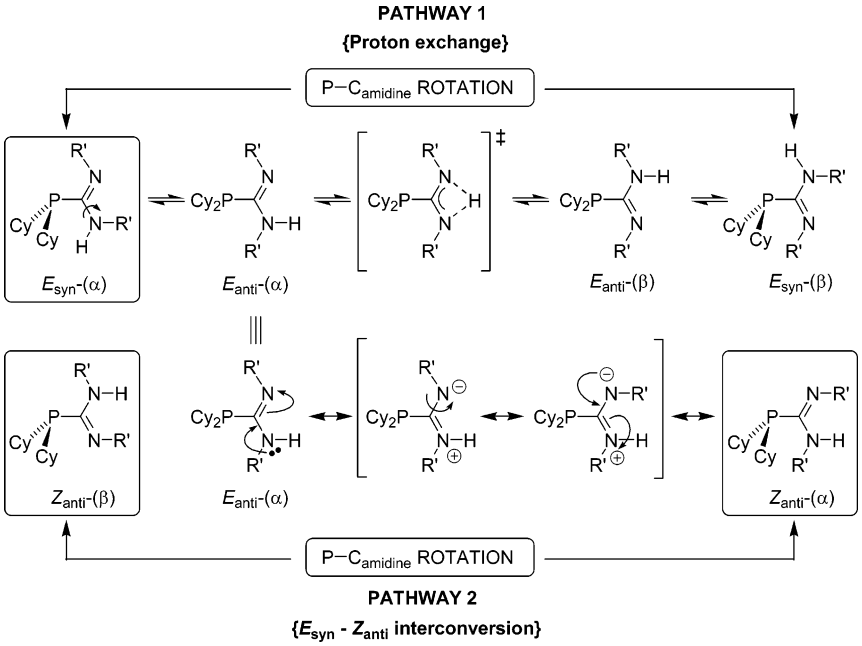

Table 1. Crystal Structure and Refinement Data for **2a**, {**3b**}, and {**4b**}

	2a	{**3b**}	{**4b**}
formula	$C_{19}H_{37}N_2P$	$C_{25}H_{33}N_2PS$	$C_{25}H_{33}N_2PSe$
formula weight	324.48	424.56	471.46
temperature (K)	173(2)	173(2)	223(2)
wavelength (Å)	0.71073	0.71073	0.71073
crystal size (mm)	0.25 × 0.20 × 0.15	0.35 × 0.30 × 0.25	0.30 × 0.30 × 0.30
crystal system	orthorhombic	monoclinic	triclinic
space group	*Pbca* (No.61)	$P2_1/c$ (No.14)	$P\bar{1}$ (No.2)
a (Å)	9.9734(3)	14.3934(2)	8.8687(1)
b (Å)	24.3803(7)	9.6078(2)	9.6892(1)
c (Å)	16.6163(4)	17.3407(3)	14.9910(2)
α (deg)	90	90	82.172(1)
β (deg)	90	100.495(1)	82.934(1)
γ (deg)	90	90	69.345(1)
V (Å^3)	4040.3(2)	2357.91(7)	1190.24(2)
Z	8	4	2
D_c (Mg m^{-3})	1.07	1.20	1.32
absorption coefficient (mm^{-1})	0.14	0.22	1.66
θ range for data collection (deg)	3.46 to 26.02	3.93 to 25.03	3.73 to 27.88
reflections collected	21806	23714	15459
independent reflections	3964 [R_{int} = 0.074]	4118 [R_{int} = 0.065]	5599 [R_{int} = 0.030]
reflections with $I > 2\sigma(I)$	2902	3539	5129
data/restraints/parameters	3964/0/203	4118/0/266	5599/0/266
goodness-of-fit on F^2	1.002	1.031	1.040
final *R* indices [$I > 2\sigma(I)$]	R1 = 0.056 wR2 = 0.136	R1 = 0.035 wR2 = 0.082	R1 = 0.025 wR2 = 0.056
R indices (all data)	R1 = 0.082 wR2 = 0.153	R1 = 0.044 wR2 = 0.087	R1 = 0.030 wR2 = 0.059
largest diff. peak and hole (e Å^{-3})	1.15 and −0.22	0.29 and −0.27	0.34 and −0.32

at early transition-metal elements,[16] which necessarily involves formation of an E_{anti} arrangement of substituents. Rotation about the C−N and C−P bonds regenerates the initial configuration via the corresponding *β*-conformer. Pathway 2 {E_{syn} − Z_{anti} interconversion} involves redistribution of electron density and formation of a zwitterionic intermediate that can conceivably occur from a number of starting configurations. As an illustration, Scheme 3 shows the process proceeding via the E_{anti}-(α) conformer, leading to the Z_{anti} isomer, which is able to convert between the α- or *β*-conformers via P−C rotation. Using spectroscopic techniques alone, it has not been possible to identify from which configuration such an electronic rearrangement is likely to occur, or indeed to determine whether Pathways 1 and 2 are independent from one another.

Crystallographic Characterization of Cy$_2$PC{N^{i}Pr}{NH^{i}Pr} (2a). The molecular structure of **2a** is illustrated in Figure 3, crystal structure and refinement data are collected in Table 1, and bond lengths and angles, along with those of {**1a**} and {**1b**} for comparison, are presented in Table 2.

As observed previously in the structurally characterized *P*-diphenyl examples {**1a**,**b**},[9] compound **2a** exists as the monomeric species in the solid state, in which a carbon-bound

(16) Mansfield, N. E.; Grundy, J.; Coles, M. P.; Hitchcock, P. B. 2006. Manuscript in preparation.

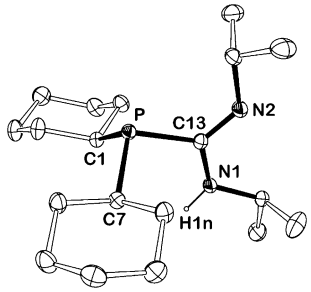

Figure 3. ORTEP representation of the molecular structure of $Cy_2PC\{N^i$-$Pr\}\{NH^iPr\}$ (**2a**). Ellipsoids drawn at the 30% probability level; hydrogens except N*H* omitted.

Table 2. Selected Bond Lengths (Å) and Angles (deg) for {**1a,b**} and **2a** (labels from Figure 3)

	{**1a**}	{**1b**}	**2a**
	Bond Lengths		
P−C(1)	1.882(3)	1.878(2)	1.882(2)
C(1)−N(1)	1.268(3)	1.286(2)	1.278(3)
C(1)−N(2)	1.372(3)	1.364(2)	1.375(3)
$P-C(R_1)$	1.835(3)	1.833(2)	1.871(2)
$P-C(R_2)$	1.835(2)	1.831(2)	1.874(2)
Δ_{CN}	0.104	0.078	0.097
	Bond Angles		
N(1)−C(1)−N(2)	120.2(2)	120.56(19)	118.39(18)
N(1)−C(1)−P	124.07(19)	122.97(14)	125.40(16)
N(2)−C(1)−P	115.63(18)	116.46(14)	116.21(14)
$C(1)-P-C(R_1)$	99.92(12)	102.05(9)	99.66(9)
$C(1)-P-C(R_2)$	101.80(11)	100.25(9)	99.04(9)
$C(R_1)-P-C(R_2)$	101.81(11)	103.44(9)	104.71(9)

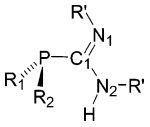

amidine unit is present with an E_{syn}-(α) configuration of substituents. The hydrogen atom on the amino nitrogen was located and refined. There are no significant differences noted in the bond lengths upon replacement of the *P*-phenyl substituents with cyclohexyl groups, with retention of the localized C−N single and C═N double bonds (Δ_{CN} = 0.097 Å),[3] consistent with the solution-state structure. In **2a** the amidine unit is rotated such that it lies in the sterically most favorable position with respect to the phosphorus substituents, with N(1)−C(13)−P−Cy torsion angles of +54.8° and −51.9° and the amino substituent located between the two cyclohexyl substituents (Figure 4). This is in contrast to the corresponding rotational position of the amidine group in the *P*-diphenyl analogues, which are aligned with one of the P−Ph bonds [N_{amine}−C−P−Ph torsion angles: {**1a**} 0.0° and −104.4°; {**1b**} 10.6° and −95.7°] (Figure 4), with short intramolecular $NH\cdots C_{ipso}$ distances of 2.33 Å and 2.42 Å noted for {**1a**} and {**1b**}, respectively. In our previous communication we postulated that this seemingly sterically unfavorable twist was due to an attractive interaction between the amino proton and the aromatic π-cloud of the phenyl substituent. In an attempt to probe the causes behind this structural characteristic, and other features associated with this class of molecules, DFT calculations have been carried out on representative model complexes.

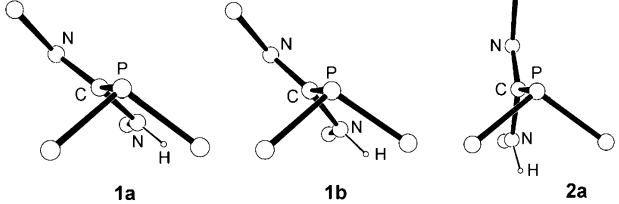

Figure 4. View of the core atoms of compounds {**1a**,**b**} and **2a** showing the relative rotation of the amidine unit about the P−C vector.

DFT Studies on Model Phospha(III)guanidine Compounds. Examples of model phospha(III)guanidine compounds have been examined using the B3LYP density functional theory and the 6−31g(d) basis set, implemented by Gaussian 03.[17] Initial calculations were performed on the E_{syn}-(α) isomers of the *N*-methyl substituted models $Ph_2PC\{NMe\}\{NHMe\}$ (**A**) and $Cy_2PC\{NMe\}\{NHMe\}$ (**B**), where the reduced complexity of the nitrogen substituents was employed to lower their steric impact, thus highlighting any significant electronic contributions to the calculated geometries. Discrepancies between the bond lengths and angles of the fully optimized geometries and the observed crystal structure data were typically within a 2% margin of error. It was noted, however, that the computed geometry at the N_{amine} atom indicated a greater pyramidalization than observed in the crystallographic data, as shown by the DP-(%) values[12] [**A** = 5.5 cf. **1a** = 0.4 and **1b** = 0.3; **B** = 9.6 cf. **2a** = 1.9], which may reflect an underestimation in the delocalization of the nitrogen lone pair within the amidine unit.

In both cases **A** and **B**, the HOMO contains considerable lone-pair character at the phosphorus atom, in agreement with our recent experimental results in which it has been shown that these ligands will coordinate as Lewis bases via the phosphorus to late transition-metal centers.[8] Despite the apparent underestimation in the delocalization of the N_{amine} lone pair inferred from the geometry at this atom, a significant stabilization arises from overlap with the $C{=}N_{imine}$ π*-orbital in both models, while the main stabilizing influence associated with the N_{imine} lone pair is from overlap with the P−C σ*-orbital. In **A**, stabilization of the phosphorus lone pair arises predominantly through delocalization into the antibonding orbitals of the phenyl substituents, which accounts for the observed difference in natural charge on the phosphorus atom of **A** [+0.83] compared with **B** [+0.78], where no such delocalization is possible in this system.

The origin of the preferentially canted amidine unit in the *P*-diphenyl derivatives (Figure 4) was examined using model compound **A**. Using an initial conformation in which the amidine unit had been rotated about the P−C bond such that it bisected that Ph−P−Ph angle [N_{amine}−C−P−C_{ipso} torsion angle: ±53.14°] and allowing full optimization, the molecule minimized to a geometry in which the N_{amine} group eclipsed one of the phenyl substituents [final torsion angles: −9.31° and −114.92°], indicating that the preference for this orientation cannot be solely a result of crystallographic forces in the solid state. NBO analysis of the minimized structure did not indicate any significant interaction between the N*H* and the phenyl substituents in **A**, as postulated in the original publication. However, it is noted that molecular orbitals 54a and 53a (corresponding to the HOMO−14 and HOMO−15) indicate overlap between the amino group and the π-system of the

(17) Frisch, M. J.; et al. *Gaussian 03*, revision 03W; Gaussian, Inc.: Wallingford CT, 2004.

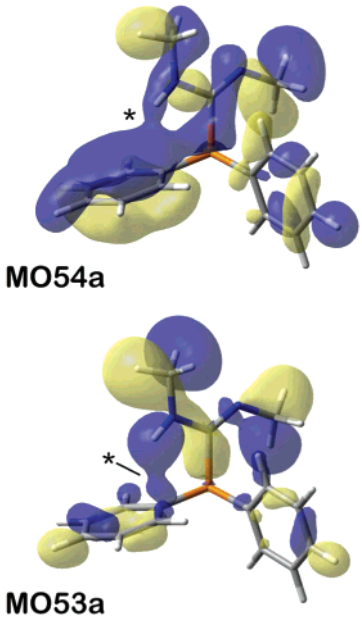

Figure 5. MO54a and MO53a of **A** (constructed with isovalues at 0.02) indicating positive overlap (*) between the amino component of the amidine and the π-system of an aromatic substituents on phosphorus.

proximate phenyl substituents that may contribute to the stabilization of this arrangement (Figure 5).

To help further our understanding of the fluxional processes determined to be occurring in solution (vide supra), it was of interest to compare the relative energies the eight configurations illustrated in Scheme 2. Full geometry optimizations were performed for model compounds **A** and **B** in which the torsion angle for the amidine unit was arbitrarily set to approximate the (α) and (β) conformations (Figure 6). In agreement with the experimental data, the E_{syn}-(α) conformer proved to be the minimum energy structure for both **A** and **B**, with the highest energy calculated for the sterically unfavorable Z_{syn}-(α) arrangement. Assuming the interchange of the nitrogen substituents observed in the ^{1}H NMR spectra proceeds via the proton exchange mechanism proposed in Scheme 3 [i.e. E_{syn}-(α) $\leftrightarrow$ E_{anti}-(α) $\leftrightarrow$ E_{anti}-(β) $\leftrightarrow$ E_{syn}-(β)], a pathway involving higher-energy isomers is calculated for the *P*-diphenyl model **A**, in agreement with the observation that this process only occurs at elevated temperature. Interestingly, relatively low-energy structures are noted for the Z_{syn}-(β) and Z_{anti}-(β) configurations of **B**, suggesting that the minor isomer of **2a**, spectroscopically identified as containing the amidine unit in the Z_{anti} form, is likely to be the β-conformer.

Synthesis and Structure of Phospha(V)guanidines, R_2P-(E)C{NR′}{NHR′}. Oxidation of the phospha(III)guanidines {**1a**,**b**} and **2a**,**b** to the corresponding P(V)sulfide and -selenide derivatives proceeded smoothly via reaction with the elemental chalcogen, to afford Ph_2P(E)C{NR′}{NHR′} [{**3a**,**b**} E = S; {**4a**,**b**} E = Se][11] and Cy_2P(E)C{NR′}{NHR′} [**5a**,**b** E = S; **6a**,**b** E = Se] (Scheme 1).[18] Compounds **3**−**6** were purified by crystallization from hot heptane, affording the target species in good to excellent yields (61−95%).

Comparable NMR spectroscopic data are observed for each of the *P*-diphenyl derivatives, irrespective of the chalcogen and nitrogen substituents, and it is therefore assumed that similar solution-state behavior occurs in all cases. In this instance, the N-*Cy* compound {**4b**} was selected for a detailed NMR study. The ^{1}H NMR spectrum of {**4b**} (Figure 7) contains two low-field multiplets (**a** and **b**), corresponding to the ortho C_6H_5 protons of two distinct species that were shown, through spin saturation transfer experiments, to form an equilibrium mixture. Further evidence for these two species is given by four resolved resonances for the α-*H* of the cyclohexyl groups (**e**−**h**), consistent with inequivalent *N*-substituents within the amidine unit of each form. The major N*H* resonance (**d**) at δ 5.42 is present as an unresolved doublet of doublets, exhibiting three-bond coupling of similar magnitude to both phosphorus and the α-C*H* of the N_{amine}-substituent; spin saturation transfer experiments indicate this peak to be in exchange with an additional pseudotriplet at δ 6.96 (**c**), obscured by the aromatic resonances. Selective decoupling experiments were implemented to pair the N_{imine} and N_{amine} α-C*H* resonances, and while selective irradiation of the multiplet at δ 3.45 gave a signal enhancement for the corresponding multiplet at δ 3.65, no such enhancement was observed between the remaining two signals, due to more pronounced localization of the carbon−nitrogen single and double bonds in this isomer. nOe experiments showed that, upon irradiation of the ortho phenyl protons (**a**), the only enhancement observed corresponded to other aromatic resonances, while irradiation of (**b**) resulted in enhancement of both (**d**) and (**f**), corresponding to N*H* and α-C*H* groups, respectively. This suggests free rotation about the P−CN_2 bond in one of the solution-state species and a "locked" geometry in the other.

The ^{31}P{^{1}H} NMR spectrum of {**4b**} shows two well-separated resonances at δ 36.0 and δ 24.3 in 1.0:1.3 ratio (Table 3). Each peak displays selenium satellites with J_{SeP} values of −721 and −753 Hz, respectively; the corresponding doublets in the ^{77}Se{^{1}H} NMR spectrum resonate at δ −223.6 (−721 Hz) and δ −310.9 (−753 Hz). It is noted that in the ^{1}H coupled ^{77}Se experiment, the lower frequency resonance exhibits a further coupling of 6 Hz, which is removed upon selective decoupling of the N*H* resonance (**c**). The magnitude of this coupling is less than predicted for a direct Se−H bond (typical values: $^1J_{SeH} \approx 50$ Hz; $^2J_{SeH}/^3J_{SeH} \approx 10-20$ Hz)[19] suggesting a hydrogen-bonding interaction between the selenium atom and the amino proton. Similar intramolecular contacts have afforded J_{SeH} values of around 12−13 Hz,[20] indicating that this is likely to be a weak Se···H interaction in {**4b**}. It is noted, however, that this interaction is evidently strong enough to slow rotation about the P−$C_{amidine}$ bond on the NMR time scale to generate the "locked" conformation, as described above. In summary, these spectroscopic data for {**4b**} present strong evidence for the existence of E_{syn} and Z_{syn} amidine configurations in solution, which are both present as the β-conformers.

Variable-temperature NMR studies of {**4b**} show that below 248 K the relative amounts of E_{syn}-(β):Z_{syn}-(β) isomers in solution are constant at 2.5:1.0, representing the thermodynamic ratio between these two isomers. Upon raising the temperature above 248 K, the relative amount of Z_{syn}-(β) increases to give the 1.3:1.0 ratio observed at 298 K. Van't Hoff analysis of the data between 248 and 298 K gives a value of ΔH of 2.7 kcal

(18) Attempted synthesis of the corresponding phosphine oxides of **1b** using *tert*-butyl peroxide resulted in cleavage of the phosphorus−carbon bonds and isolation of the hydrogen-bonded ion-pair, [HC{NHCy}$_2$][Ph_2PO_2]. Mansfield, N. E.; Coles, M. P.; Hitchcock, P. B. Unpublished results.
(19) McFarlane, W.; Wood, R. J. *J. Chem. Soc., Dalton Trans.* **1972**, 1397.
(20) Wu, R.; Hernández, G.; Odom, J. D.; Dunlap, R. B.; Silks, L. A. *Chem. Commun.* **1996**, 1125.

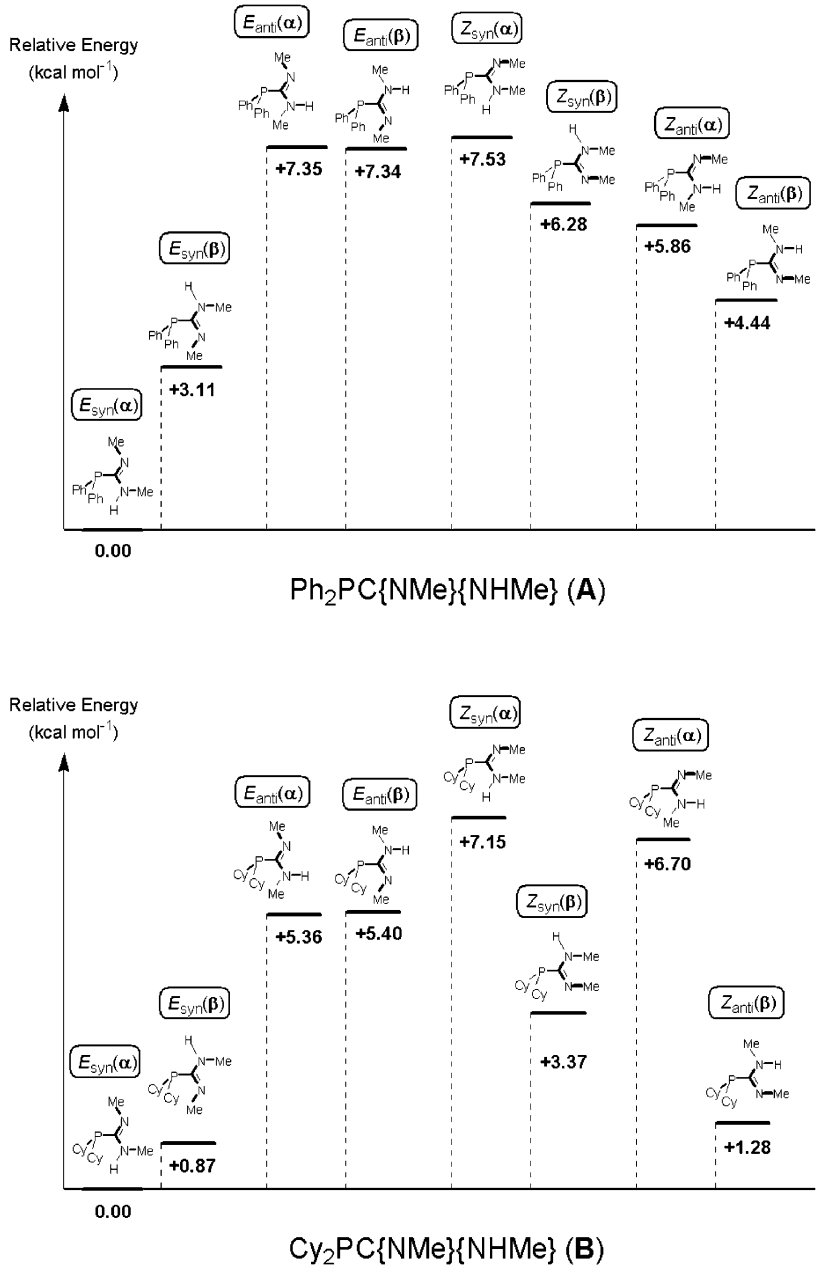

Figure 6. Graph of the relative energies of the optimized structures of $Ph_2PC\{NMe\}\{NHMe\}$ (**A**) and $Cy_2PC\{NMe\}\{NHMe\}$ (**B**) considering the eight different configurations, as described in Scheme 2.

mol^{-1} with the corresponding entropy value calculated at +9.1 eu. Assuming that a mechanistic pathway similar to that outlined in Scheme 3 is operating for the E_{syn}-to-Z_{syn} isomerization (involving generation of a zwitterionic intermediate), the increased energy assoicated with this process compared to that associated with **2a** may reflect a decreased tendency for the amino nitrogen to assume a positive charge, due to overlap with the lone pairs of the chalcogen atom (vide infra).

As observed for the P(III) systems described above, changing the phosphorus substituents from phenyl to cyclohexyl has a large impact on the configuration of the amidine unit, despite the distance between these groups within the molecule. To illustrate these differences, the spectroscopic features associated with the corresponding *P*-dicyclohexyl complex, $Cy_2P(Se)C\{NCy\}\{NHCy\}$, **6b**, are described. The $^{31}P\{^1H\}$ NMR spectrum of **6b** also shows two resonances [δ 62.7 and δ 66.4], although for this compound the ratio of the two species is heavily biased toward one isomer, with a ratio of ~19:1. As for {**4b**}, the ^{77}Se resonance corresponding to the major isomer exhibits a large $^1J_{SeP}$ coupling of −690 Hz and a small J_{SeH} coupling of 6 Hz, which disappears on selective decoupling of the N*H* resonance (Figure 8).

The ^1H NMR spectrum of **6b** reflects this change in the relative ratio of species present in solution, with resonances for the major isomer dominating the spectra, such that the low-intensity signals of the minor isomer were difficult to assign. The N*H* resonance of the major species is observed as a poorly defined doublet of doublets at δ 6.90, with two resolved multiplets for the α-C*H* of the *N*-cyclohexyl substituents, again consistent with localized bonding in the amidine. nOe's are observed between both *N*-cyclohexyl groups, and between the N_{amine} substituent and the N*H* proton, consistent with the major

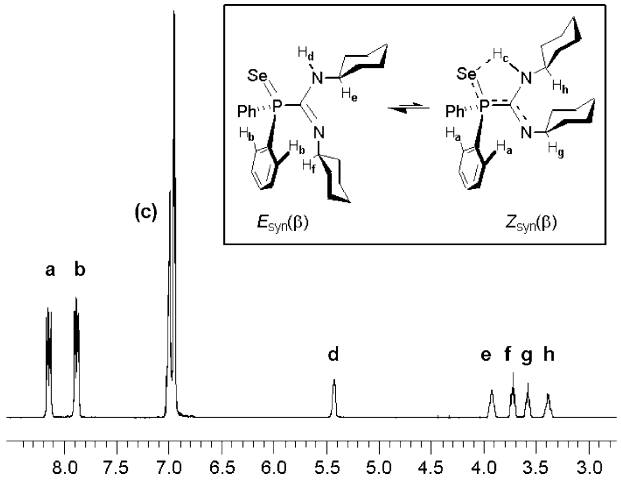

Figure 7. ^{1}H NMR spectrum of {**4b**} (500 MHz, [^{2}H]$_8$-toluene, 293 K) showing the aromatic and cyclohexyl α-C*H* regions.

Table 3. Summary of ^{31}P NMR Data (121.4 MHz, [^{2}H]$_6$-benzene, 298 K) for **3**−**6**

compound	major resonance (J_{PSe})	minor resonance (J_{PSe})	relative ratio (293 K)[a]
{**3a**}	δ 33.6	δ 38.2	1.6:1.0
{**3b**}	δ 34.0	δ 38.6	1.2:1.0
{**4a**}	δ 23.2 (−755 Hz)	δ 35.2 (−721 Hz)	1.5:1.0
{**4b**}	δ 23.9 (−753 Hz)	δ 35.5 (−721 Hz)	1.3:1.0
5a	δ 63.3	δ 67.4	8.4:1.0
5b	δ 63.7	δ 67.0	18.0:1.0
6a	δ 62.4 (−692 Hz)	δ 67.0[b]	14.6:1.0
6b	δ 62.7 (−690 Hz)	δ 66.4[b]	19.0:1.0

[a] Relative ratio of isomers calculated from integration of ^{31}P NMR resonances. [b] J_{PSe} could not be detected due to the low relative intensity of the signal.

isomer in this case being the Z_{syn}-(β). These data therefore indicate an almost complete shift in the equilibrium for the *P*-dicyclohexylphospha(V)guanidines to the theoretically most sterically unfavorable Z_{syn} isomer in solution.

It is worthwhile noting that in the ^{1}H NMR spectra of the P(V) system, the N*H* resonance is present as a (poorly resolved) pseudotriplet in both the E_{syn}-(β) and Z_{syn}-(β) isomers of {**4b**} and the observable Z_{syn}-(β) isomer of **6b**. Comparing these data to the spectra of the P(III) derivatives {**1a**,**b**}[9] and **2a**,**b** (vide supra), the corresponding N*H* resonance for the E_{syn}-(α) configuration is observed as a doublet, with no coupling to the phosphorus. Given that the N*H* resonance of the Z_{anti} configuration of **2a** is present as a well-defined (albeit broad) pseudotriplet with resolvable $^3J_{HP}$ coupling (Figure 2), and that the DFT analysis indicated an energy profile of in favor of the β-conformation of the Z_{anti} isomer, we assign the minor isomer in the *P*-dicyclohexylphospha(III)guanidines as corresponding to the β-conformation.

NMR spectroscopic data also indicate differences in the distribution of electron density depending on the configuration of the amidine, indicated by changes in the J_{PC} values. An unusually large $^1J_{PC}$ coupling of 123 Hz is observed to the P*C*N$_2$ in the Z_{syn}-(β) isomer of {**4b**}, approximately 3 times the corresponding value in the E_{syn}-(β) isomer [43 Hz] and the *P*-diphenyl phospha(III)guanidines [32 Hz]; a similarly large value of 107 Hz is noted in **6b**. Also, $^3J_{PC}$ coupling is observed to the α-*C*H of both N-substituents in the Z_{syn} isomers of {**4b**} and **6b**, while this coupling is only observed through the C═N bond in the corresponding P(III) analogues.

The infrared spectra of {**1b**}, {**4b**}, and **6b** have also been recorded in $CDCl_3$ solution (Figure 9). The υ(N−H) of {**1b**}, in which no hydrogen bonding involving the N*H* is observed using other spectroscopic or solid-state analytical techniques, was identified as a strong absorption at 3427 cm^{-1} (Figure 9a). In agreement with NMR data, two isomeric forms of {**4b**} have been identified (Figure 9b), with broad absorptions at 3304 and 3262 cm^{-1} assigned to υ(N−H···Se) and a sharp signal observed at 3428 cm^{-1} for the terminal υ(N−H). To corroborate these assignments, the corresponding IR of the cyclohexyl derivative **6b**, in which the predominant isomer involves intramolecular N−H···Se interactions, only shows the bathochromically shifted N*H* absorption at 3251 cm^{-1} (Figure 9c). Compared with calculated[21] [∼2550 cm^{-1}] and observed[22] [2240−2320 cm^{-1}] Se−H absorptions, these values are too high to be considered as originating from a direct Se−H bond, consistent with the postulated intramolecular hydrogen-bonding situation.

Crystallographic Study of P(V) Sulfide and Selenide Derivatives and the Borane Adduct, $Ph_2P(BH_3)C${NCy}{NHCy}. Single-crystal X-ray diffraction studies were performed on representative compounds {**3b**}, {**4b**}, **5a**, **6a**, and **6b** (Figures10 and 11); crystal structure and refinement data are collected in Table 4 and bond lengths and angles in Table 5. The molecular structure of each compound conforms to the expected formula of $R_2P(E)C\{NR'\}\{NHR'\}$, and all derivatives are monomeric with no significant intermolecular interactions. As for the P(III) derivatives discussed above, the hydrogen atom on the amino nitrogen was located and refined in each case. For all compounds, the phosphorus atom is in a distorted tetrahedral geometry, with P = E bond lengths consistent with related R_3P═S sulfides (R = Ph, 1.949−1.955 Å;[23] R = Cy, 1.966−1.961 Å[24]) and R_3P═Se selenides (R = Ph, 1.105−2.113 Å;[25] R = Cy, 2.108 Å[26]). Localized C═N double and C−N single bonds are noted within the "NCN" component, with Δ_{CN} values ∼0.08 Å.

The structurally characterized *P*-diphenyl derivatives, {**3b**} and {**4b**}, exist as the E_{syn}-(β) isomer in the solid state, corresponding to the major component identified in solution. In this configuration, the N*H* proton is located in a position that will enable interaction with the chalcogen lone pairs, with N*H*···E═P distances of 2.45 Å and 2.63 Å noted for {**3b**} and {**4b**}, respectively (within the sum of their van der Waals radii:[27] S = 1.80 Å; Se = 1.90 Å; H = 1.20 Å). These distances are within the range observed in related structures composed of five-membered rings containing such intramolecular interactions [sulfides: 2.25−2.76 Å; selenides: 2.60−2.79 Å].[28,29] To

(21) Leszczyñski, J.; Kwiatkowski, J. S. *J. Phys. Chem.* **1993**, *97*, 1364.
(22) Smith, D. M.; Ibers, J. A. *Polyhedron* **1998**, *17*, 2105; Di Vaira, M.; Peruzzini, M.; Stoppioni, P. *Inorg. Chem.* **1991**, *30*, 1001; Cui, C.; Roesky, H. W.; Hao, H.; Schmidt, H.-G.; Noltemeyer, M. *Angew. Chem., Int. Ed.* **2000**, *39*, 1815.
(23) Codding, P. W.; Kerr, K. A. *Acta Crystallogr., Sect. B* **1978**, *34*, 3785; Foces-Foces, C.; Llamas-Saiz, A. L. *Acta Crystallogr., Sect. C* **1998**, *54*, IUC9800013; Ziemer, B.; Rabis, A.; Steinberger, H.-U. *Acta Crystallogr., Sect. C* **2000**, *56*, e58.
(24) Kerr, K. A.; Boorman, P. M.; Misener, B. S.; van Roode, J. G. H. *Can. J. Chem.* **1977**, *55*, 3081; Reibenspies, J. H.; Draper, J. D.; Struck, G.; Darensbourg, D. J. *Z. Kristallogr.* **1996**, *211*, 400.
(25) Codding, P. W.; Kerr, K. A. *Acta Crystallogr., Sect. B* **1979**, *35*, 1261; Jones, P. G.; Kienitz, C.; Thone, C. *Z. Kristallogr.* **1994**, *209*, 80.
(26) Davies, J. A.; Dutremez, S.; Pinkerton, A. A. *Inorg. Chem.* **1991**, *30*, 2380.
(27) Bondi, A. *J. Phys. Chem.* **1964**, *68*, 441.
(28) Siasios, G.; Tiekink, E. R. T. *Z. Kristallogr.* **1992**, *200*, 295; Siasios, G.; Tiekink, E. R. T. *Z. Kristallogr.* **1993**, *207*, 59; Siasios, G.; Tiekink, E. R. T. *Z. Kristallogr.* **1995**, *210*, 619; Andrieu, J.; Camus, J.-M.; Poli, R.; Richard, P. *New J. Chem.* **2001**, *25*, 1015; Zhang, Q.; Ly, T.; Slawin, A. M. Z.; Woolins, J. D. *Rev. Roum. Chim.* **2002**, *47*, 1015.

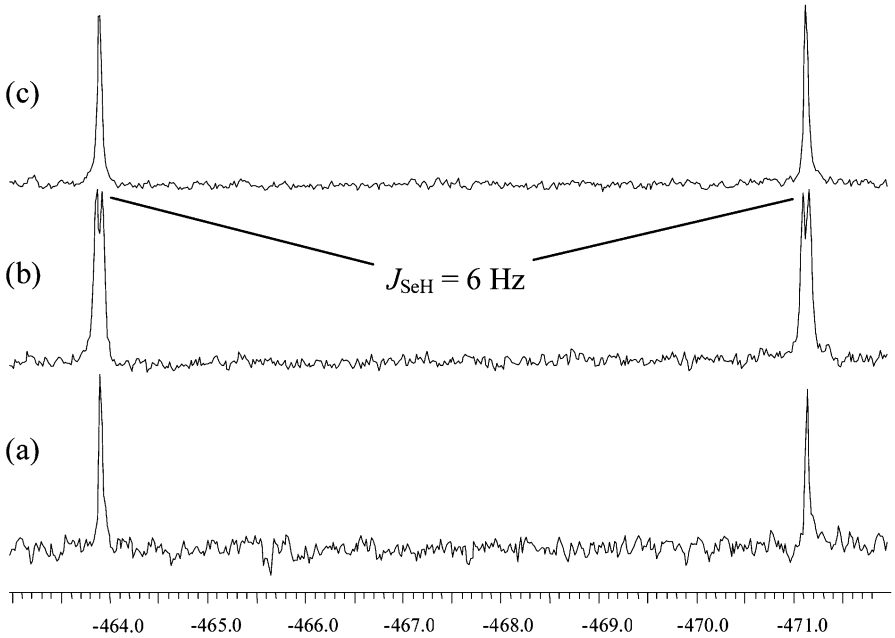

Figure 8. ^{77}Se NMR spectra of **6b** (95.3 MHz, [^{2}H]$_6$-benzene, 298 K). (a) ^{77}Se{^{1}H} spectrum. (b) ^{1}H-coupled ^{77}Se spectrum. (c) Selective decoupling of the ^{1}H resonance at δ 6.90.

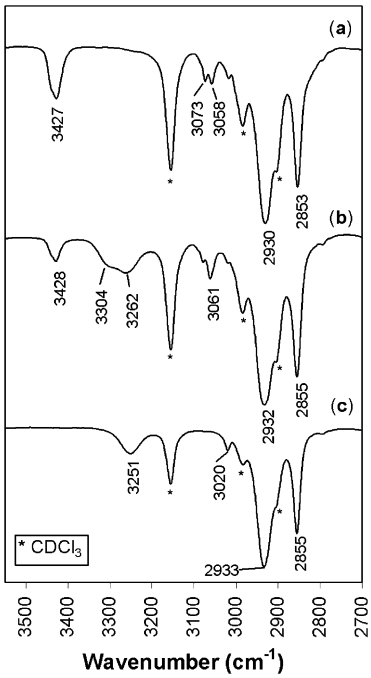

Figure 9. Solution-state IR spectra of (a) $Ph_2PC\{NCy\}\{NHCy\}$ {**1b**}; (b) $Ph_2P(Se)C\{NCy\}\{NHCy\}$ {**4b**}; (c) $Cy_2P(Se)C\{NCy\}\{NHCy\}$ **6b**.

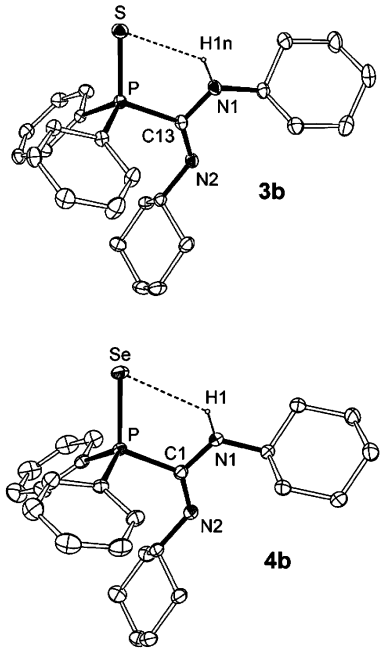

Figure 10. ORTEP representation of the molecular structures of Ph_2P-(S)C{NCy}{NHCy} {**3b**} and $Ph_2P(Se)C\{NCy\}\{NHCy\}$ {**4b**}. Ellipsoids drawn at the 30% probability level; hydrogen atoms, except N*H*, omitted.

generate a favorable alignment for this intramolecular interaction while maintaining a planar amidine unit, a small twist angle is adopted between the "E═P−C" and "N−C−N" planes, with values of 13.9° and 12.0° for {**3b**} and {**4b**}, respectively.

The sp^2-carbon of the amidine unit is planar for each of the structurally determined P(III)- and P(V)-diphenyl derivatives, with experimentally equivalent (within 3σ) "N−C═N" angles of ∼120°. However, the P(V)−C−N_{amine} angle is considerably smaller than in the corresponding P(III) compounds [av {**3b**} and {**4b**} = 110.36°; av {**1a**} and {**1b**} = 116.05°] with a corresponding increase in the P−C═N_{imine} angle [av {**3b**} and {**4b**} = 128.56°; av {**1a**} and {**1b**} = 123.52°] representing a "pitch" of the amidine unit toward the chalcogen atom. This observation may be explained considering two complimentary perspectives: using a purely steric argument, the shift in the ground-state configuration from E_{syn}-(α) to E_{syn}-(β) that occurs upon oxidation places the N_{imine} substituent in an unfavorable position with respect to the phenyl groups, causing steric repulsion to force the amidine unit to reposition itself. The alternative perspective is to consider an electronic attraction between the amine proton and the chalcogen which "pulls" the amidine unit away from the phosphorus substituents.

(29) Siasios, G.; Tiekink, E. R. T. *Z. Kristallogr.* **1995**, *210*, 868.

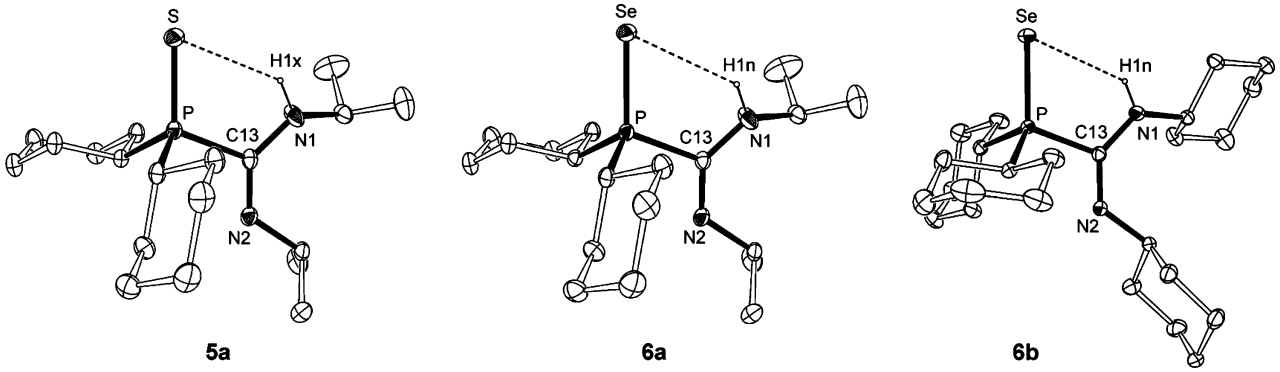

Figure 11. ORTEP representation of the molecular structures of $Cy_2P(S)C\{N^iPr\}\{NH^iPr\}$ (**5a**), $Cy_2P(Se)C\{N^iPr\}\{NH^iPr\}$ (**6a**) and $Cy_2P(Se)C\{NCy\}\{NHCy\}$ (**6b**). Ellipsoids drawn at the 30% probability level; hydrogen atoms, except N*H*, omitted.

Table 4. Crystal Structure and Refinement Data for **5a**, **6a**, **6b** and **7**

	5a	6a	6b	7
formula	$C_{19}H_{37}N_2PS$	$C_{19}H_{37}N_2PSe$	$C_{25}H_{45}N_2PSe$	$C_{25}H_{36}BN_2P$
formula weight	356.54	403.44	483.56	406.34
temperature (K)	173(2)	173(2)	173(2)	173(2)
wavelength (Å)	0.71073	0.71073	0.71073	0.71073
crystal size (mm)	0.20 × 0.20 × 0.20	0.30 × 0.30 × 0.20	0.40 × 0.40 × 0.35	0.20 × 0.15 × 0.10
crystal system	triclinic	triclinic	triclinic	monoclinic
space group	$P\bar{1}$ (No.2)	$P\bar{1}$ (No.2)	$P\bar{1}$ (No.2)	$P2_1/n$ (No.14)
a (Å)	8.9912(3)	8.9350(3)	9.9173(2)	9.1464(4)
b (Å)	10.0100(3)	10.0808(3)	10.1444(3)	15.3363(4)
c (Å)	12.4892(5)	12.5565(4)	14.1035(4)	17.7735(7)
α (deg)	77.228(2)	77.397(2)	105.398(1)	90
β (deg)	77.769(2)	78.020(2)	97.112(1)	104.714(2)
γ (deg)	76.842(2)	77.321(2)	104.885(1)	90
V (Å^3)	1051.90(6)	1061.57(6)	1293.67(6)	2411.36(16)
Z	2	2	2	4
D_c (Mg m^{-3})	1.13	1.26	1.24	1.12
absorption coefficient (mm^{-1})	0.23	1.85	1.53	0.13
θ range for data collection (deg)	3.46 to 26.10	3.45 to 26.01	3.52 to 26.08	3.80 to 25.04
reflections collected	14392	14137	21177	20602
independent reflections	4138 [R_{int} = 0.049]	4158 [R_{int} = 0.039]	5083 [R_{int} = 0.042]	4223 [R_{int} = 0.061]
reflections with $I > 2\sigma(I)$	3401	3695	4421	3253
data/restraints/parameters	4138/0/212	4158/0/212	5083/0/266	4223/0/278
goodness-of-fit on F^2	1.016	1.040	0.944	1.040
final *R* indices [$I > 2\sigma(I)$]	R1 = 0.037	R1 = 0.029	R1 = 0.030	R1 = 0.045
	wR2 = 0.083	wR2 = 0.065	wR2 = 0.071	wR2 = 0.094
R indices (all data)	R1 = 0.050	R1 = 0.036	R1 = 0.039	R1 = 0.068
	wR2 = 0.089	wR2 = 0.067	wR2 = 0.075	wR2 = 0.104
largest diff. peak and hole (e Å^{-3})	0.25 and −0.21	0.40 and −0.42	0.33 and −0.29	0.20 and −0.23

In contrast to the *P*-diphenyl derivatives, structural characterization of **5a**, **6a**, and **6b** indicates that the Z_{syn}-(*β*) form is more stable in the solid state (Figure 11). This configuration is observed for examples containing sulfide and selenide groups (with the configuration in the latter derivatives shown to be independent of nitrogen substituent) indicating that the origin of this difference derives from the *P*-cyclohexyl groups. Structurally characterized examples of the Z_{syn} form of an amidine are unusual, usually being restricted to those in which the *C*-substituent of the NCN unit is bulky, such as in the *C*-triptycenyl[30] and *C*-*ter*-phenyl derivatives.[30,31]

In this configuration, the chalcogen and amine protons of the phospha(V)guanidines are still able to interact, with intramolecular N*H*···E═P distances of 2.54, 2.68, and 2.70 Å for **5a**, **6a**, and **6b**, respectively. While these are within the range previously noted for related *P*-dicyclohexyl sulfides [2.40−2.63 Å],[32] they lie toward the long end of the range for the corresponding selenides [2.37−2.65 Å].[29,33]

To accommodate the close proximity of the two nitrogen substituents in the Z_{syn} form, several structural differences are noted compared to the E_{syn} isomers observed for the *P*-diphenyl compounds (Figure 12). The amine nitrogen generally exhibits a more pronounced pyramidalization in the *P*-dicyclohexyl compounds, with a increased DP(%) at the N_{amine} atom [**5a** = 7.5; **6a** = 8.6; **6b** = 2.5] compared with the *P*-diphenyl analogues [{**3b**} = 1.4; {**4b**} = 1.2]. This is most clearly observed in the displacement of the N_{amine} substituent from the NCN plane, with the resultant angle between the C−N_{amine}−R and C═N_{imine}−R planes showing considerable variation through the series of compounds [{**3b**} = 6.2°; {**4b**} = 19.4°; **5a** = 34.1°; **6a** = 38.2°; **6b** = 23.4°]. The different substituent arrangement also manifests itself in an increased N−C−N angle

(30) Baker, R. J.; Jones, C. *J. Organomet. Chem.* **2006**, *691*, 65.
(31) Schmidt, J. A. R.; Arnold, J. *J. Chem. Soc., Dalton Trans.* **2002**, 2890.
(32) Siasios, G.; Tiekink, E. R. T. *Z. Kristallogr.* **1994**, *209*, 885; Horn, E.; Kurosawa, K.; Tiekink, E. R. T. *Acta Crystallogr., Sect. E* **2001**, *57*, o321.
(33) Kramolowsky, R.; Sawluk, J.; Siasios, G.; Tiekink, E. R. T. *Z. Kristallogr. - New Cryst. Struct.* **1998**, *213*, 45.

Table 5. Selected Bond Lengths (Å) and Angles (deg) for {**3b**}, {**4b**}, **5a**, and **6a,b** (labels from Figure 10)

	{3b}	{4b}	5a	6a	6b
		Bond Lengths			
P═E	1.9536(6)	2.1183(4)	1.9690(6)	2.1237(5)	2.1207(5)
E···H	2.45	2.63	2.54	2.68	2.70
P−C(1)	1.8909(16)	1.8811(14)	1.8601(16)	1.864(2)	1.862(2)
C(1)−N(1)	1.279(2)	1.2785(18)	1.270(2)	1.270(3)	1.273(2)
C(1)−N(2)	1.361(2)	1.3602(18)	1.356(2)	1.348(3)	1.358(2)
P−C(R_1)	1.8103(15)	1.8108(14)	1.8273(16)	1.831(2)	1.839(2)
P−C(R_2)	1.8061(16)	1.8131(14)	1.8357(15)	1.839(2)	1.822(2)
Δ_{CN}	0.082	0.082	0.086	0.078	0.085
		Bond Angles			
N(1)−C(1)−N(2)	121.18(15)	120.95(13)	133.27(16)	133.07(19)	134.89(18)
E−P−C(1)	111.05(6)	112.37(4)	111.58(5)	111.45(6)	112.67(6)
E−P−C(R_1)	111.17(6)	110.19(5)	114.36(6)	114.11(6)	111.59(6)
E−P−C(R_2)	112.55(6)	111.98(4)	112.59(5)	112.45(7)	114.32(6)
N(1)−C(1)−P	129.16(12)	127.96(11)	112.45(11)	111.93(13)	111.02(13)
N(2)−C(1)−P	109.64(12)	111.07(12)	114.17(12)	114.82(15)	114.05(13)
C(1)−P−C(R_1)	106.09(7)	106.32(6)	104.14(7)	104.31(8)	106.46(9)
C(1)−P−C(R_2)	108.47(7)	105.19(6)	106.02(7)	106.23(9)	103.02(8)
C(R_1)−P−C(R_2)	107.22(7)	110.55(6)	107.48(7)	107.68(8)	108.14(8)

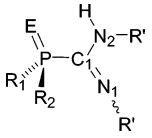

of 133.74° (av) for the *P*-dicyclohexyl species compared with 121.06 (av) in the *P*-diphenyl derivatives, with a corresponding decrease in the N_{imine}═C−P angle noted in the former compounds.

The observed change in the configuration of the amidine unit, which is dependent on the nature of the phosphorus substituents, is likely to derive from a combination of repulsive steric interactions with the N_{imine} group and an increase in the attractive force between the amine proton and the chalcogen. The latter electronic effect may be rationalized in terms of an increased stabilization of the zwitterionic $P^{(+)}-E^{(-)}$ resonance form by the electron-donating cyclohexyl substituents, augmenting the negative charge at the chalcogen which in turn enhances the N*H*···E═P interaction.

To help evaluate the steric factors that contribute to these structural changes in the amidine configuration, the borane

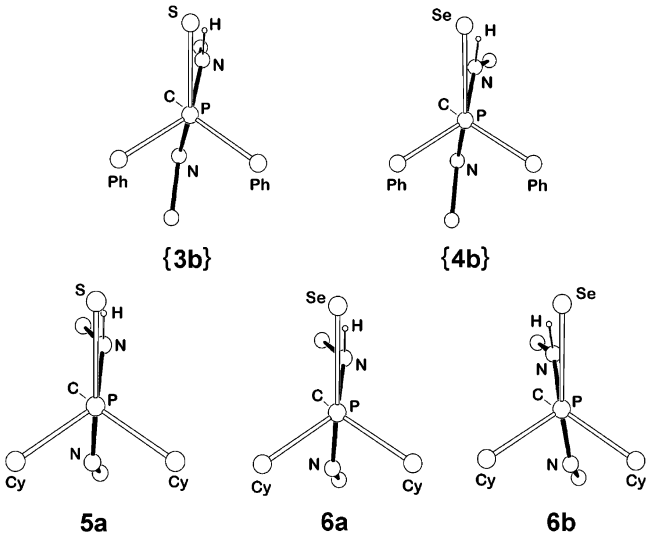

Figure 12. View of the core of P(V) phosphaguanidine compounds along the P−C vector, illustrating the structural variation in the position of the nitrogen substituents.

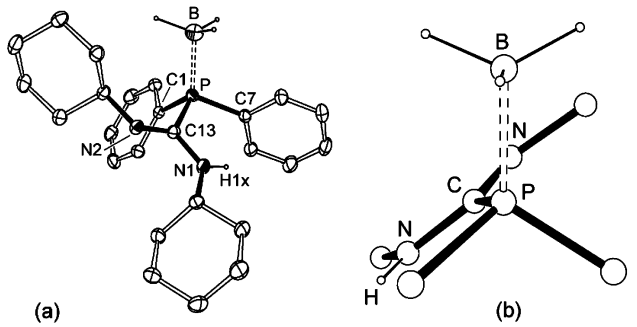

Figure 13. (a) ORTEP representation of the molecular structure of **7**. Ellipsoids drawn at the 30% probability level; hydrogen atoms except N*H* and BH_3, omitted. (b) View of the core atoms of **7** showing the relative rotation of the amidine unit about the P−C vector.

Table 6. Selected Bond Lengths (Å) and Angles (deg) for **7**

P−B	1.905(3)	P−C(13)	1.8737(19)
C(13)−N(2)	1.280(3)	C(13)−N(1)	1.367(3)
P−C(1)	1.8154(19)	P−C(7)	1.8195(19)
Δ_{CN}	0.087		
N(1)−C(13)−N(2)	120.51(18)	B−P−C(13)	114.06(11)
B−P−C(1)	117.31(11)	B−P−C(7)	110.98(11)
N(1)−C(13)−P	114.10(14)	N(2)−C(13)−P	125.37(15)
C(13)−P−C(1)	103.29(8)	C(13)−P−C(7)	104.41(9)
N(1)−C(13)−N(2)	120.51(18)	C(1)−P−C(7)	105.61(9)

adduct $Ph_2P(BH_3)C\{NCy\}\{NHCy\}$ (**7**) was prepared and structurally characterized. It was reasoned that the BH_3 group at phosphorus would exert a steric role in this position, while not being involved in any attractive intramolecular interactions with the amino N*H* group. The compound was synthesized by the combination of the P(III) starting reagent {**1b**} with a solution of the THF adduct of BH_3, and the product was crystallized from hexane in low yield. While IR (Nujol mull, CsI), elemental analysis, and X-ray diffraction studies were consistent with the formulation of **7** as the borane adduct [υ(B−H) 2395 cm^{-1} (br); υ(P−B) 565 cm^{-1} (sh)], all attempts at acquiring solution-state spectroscopic data were unsuccessful, with apparent loss of the borane and regeneration of {**1b**}, precluding any comparison of solution-state behavior between **7** and the phospha(V)-guanidines.

The molecular structure of **7** determined by X-ray crystallography (Figure 13, Tables 4 and 6) indicates that the amidine component of compound **7** adopts an E_{syn}-(α) configuration in the solid state, as noted for the previously reported *P*-diphenyl phospha(III)guanidines {**1a**} and {**1b**}. Once again localized bonding is observed in the amidine component (Δ_{CN} = 0.087 Å), with the amine N*H* orientated toward the *ipso*-carbon of one of the phenyl substituents [N_{amine}−C−P−Ph torsion angles: −2.4° and 107.9°] and an intramolecular N*H*···C_{ipso} distance of 2.38 Å.

The estimated cone angles of the P═E and P−B−H groups for {**3b**}, {**4b**}, and **7**, calculated using bond lengths from crystallographic data and van der Waals radii taken from ref 27, are 134°, 128°, and 118°, respectively, indicating that the steric influence of the borane is less than that of the sulfide or selenide substituents. This may be insufficient to cause a conformational change of the amidine to change from E_{syn}-(α) to E_{syn}-(β) that, in addition to the lack of any attractive intramolecular forces, explains the observed configuration in **7**. As for the P(III) compounds described above, DFT calcula-

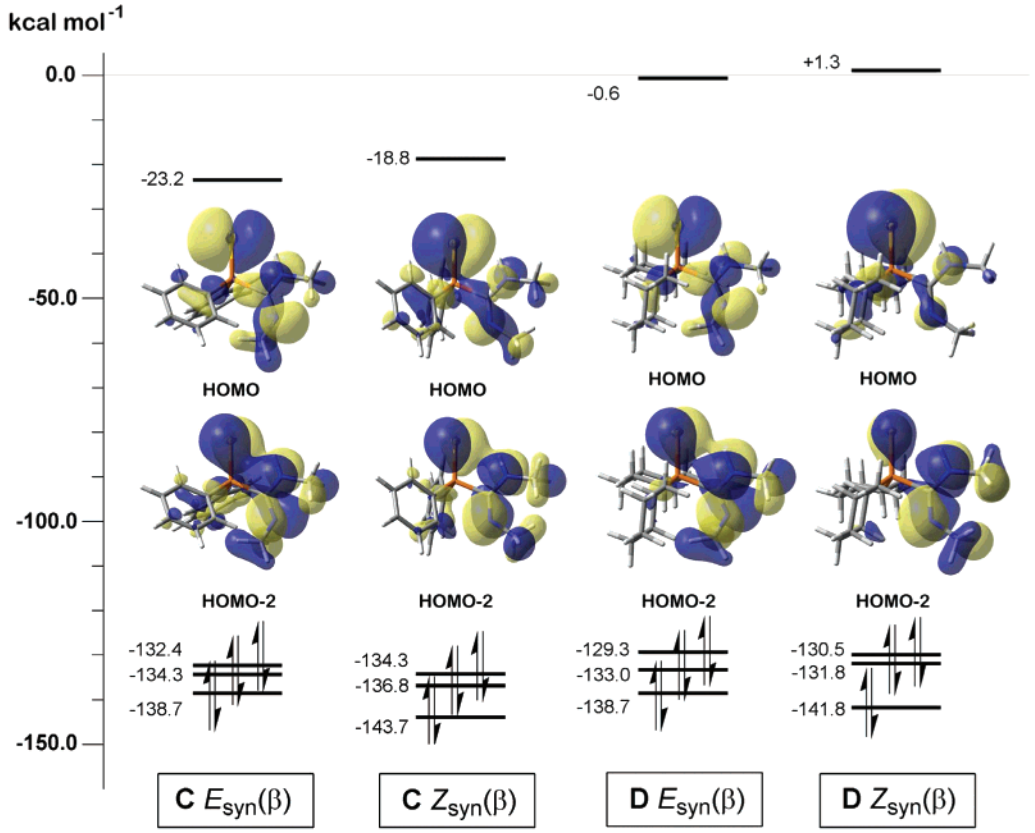

Figure 14. Orbital energy diagram for the model complexes, $Ph_2P(S)C\{NMe\}\{NHMe\}$ (**C**) and $Cy_2P(S)C\{NMe\}\{NHMe\}$ (**D**) [E_{syn}-(β) and Z_{syn}-(β) conformations], illustrating the HOMO and the HOMO−2 (constructed with isovalues at 0.02).

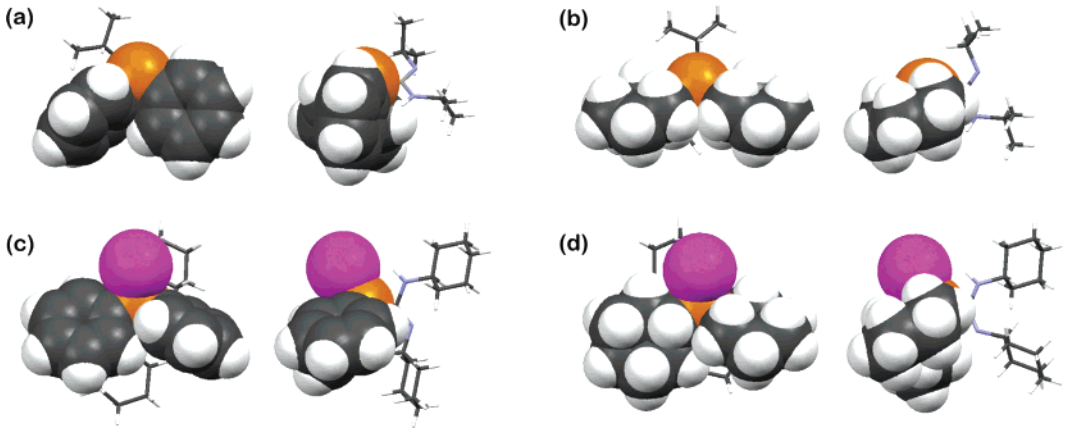

Figure 15. Spacefilling models of the phosphine moiety of phospha(III)- and phospha(V)guanidines, viewed along (left) and perpendicular (right) to the P−C vector (coordinates taken from X-ray crystallographic data). (a) $Ph_2PC\{N^iPr\}\{NH^iPr\}$, {**1a**}; (b) $Cy_2PC\{N^iPr\}\{NH^iPr\}$, **2a**; (c) $Ph_2P(Se)C\{NCy\}\{NHCy\}$, {**4b**}; (d) $Cy_2P(Se)C\{NCy\}\{NHCy\}$, {**6b**}.

tions have been utilized to help gain further insight into these structural preferences.

Molecular Modeling Studies on Phospha(V)guanidines. Using a similar approach to that employed for the P(III) compounds described above, the representative models $Ph_2P(S)C\{NMe\}\{NHMe\}$ (**C**) and $Cy_2P(S)C\{NMe\}\{NHMe\}$ (**D**) have been examined using DFT. Calculations were performed on the E_{syn}-(β) and Z_{syn}-(β) isomers of the *P*-diphenyl and *P*-dicyclohexyl sulfide models to engender further information on the differences between these two isomers. Once again, discrepancies between the bond lengths and angles of the fully optimized geometries and the observed crystal structure data were typically within a 2% threshold, indicating a good correlation between the experimental and theoretical data.

Figure 14 compares selected molecular orbitals for **C** and **D** in both the E_{syn} and Z_{syn} isomeric forms of the β-conformer. The HOMOs are similar in all cases and show significant electron density associated with a lone pair on the sulfur atom, indicating the possibility of utilizing this atom in the coordination chemistry of these species, as previously observed with the application of $Ph_3P{=}S$ as a ligand.[34] The HOMO−2 orbital contains a significant overlap between a lone pair localized on the sulfur atom and a π-symmetry component associated with the N_{amine} group, suggesting that this orbital is important in

stabilizing the (β) isomer favored in the P(V) system. This orbital is comparable in its makeup for all four examples investigated using this method, with the through space overlap between these groups appearing to be slightly more pronounced in the E_{syn} configuration for both the *P*-diphenyl and *P*-dicyclohexyl model compounds.

As indicated above, the contribution from the zwitterionic form of the phosphorus−chalcogen double bond was considered as playing a potentially important role in determining the strength of the nonbonding interaction to the amino hydrogen. Given that the solution-state data indicate a strong preference for the Z_{syn}-(β) configuration of the *P*-dicyclohexyl species in solution, it is encouraging to note that this arrangement of substituents in **D** gives the largest positive and negative values for the natural charges at phosphorus [+1.40] and sulfur [−0.66]. The charges associated with these atoms in the remaining models, however, do not indicate any clear trends that can be correlated to the experimental observations.

Overall the results from these DFT calculations are very similar, irrespective of the phosphorus substituent and the configuration of the amidine group. There does not appear to be a compelling electronic argument derived from these models as to why the *P*-dicyclohexyl compounds prefer to exist in the sterically more encumbered Z_{syn} configuration. It is likely, therefore, that steric factors play an important role in determining the subtle energetic differences that determine whether E_{syn} or Z_{syn} is the predominant form in solution, illustrated in the space filling models in Figure 15. It is, however, noted that the aforementioned S···N_{amine} overlap in the HOMO−2 of **C** and **D** is the most likely cause of the preferential adoption of the (β)-conformation in the phospha(V)guanidines that are the subject of this study.

Summary

In this work we report the synthesis of the novel phospha(III)guanidines $Cy_2PC\{NR'\}\{NHR'\}$ (R′ = ^{i}Pr, Cy) and their conversion to the corresponding sulfo- and selenophospha(V) derivatives. Analysis by NMR spectroscopy indicated that at room temperature, these compounds exist as a mixture of the E_{syn}-(α) configuration and a minor component in which the Z_{syn} arrangement of substituents is present; this latter isomer cannot be definitively assigned as the (α) or (β) conformer on the basis of spectroscopy alone. A mechanism for the interconversion of the different isomeric forms is proposed, and using model systems, DFT analysis of the relative energies of the different configurations is in agreement for a higher-energy process for the *P*-diphenyl derivative. Evidence from computational studies is also presented to explain the observation that in the *P*-diphenyl-substituted compounds, the amidine unit is rotated such that the N*H* amino group is in close proximity to one of the aromatic rings.

We have also demonstrated that amidine components of the sulfo- and selenophospha(V)guanidines containing both phenyl- and cyclohexyl-substituted phosphorus exist as a mixture of E_{syn}-(β) and Z_{syn}-(β) configurations in solution, with a strong bias toward the latter arrangement in the *P*-dicyclohexyl species. X-ray diffraction analyses reflect this trend, with examples of *P*-diphenyl compounds crystallizing with the amidine in the E_{syn}-(β) configuration, while selected *P*-dicyclohexyl analogues are shown to exist with the Z_{syn}-(β) in the solid state. In both cases, nonbonding interactions between the chalcogen and the amino hydrogen atom are noted that, on the basis of J_{Se}···H coupling in the ^{77}Se NMR spectra and the observation of multiple υ-(N−H) absorptions, are shown to be present in solution. DFT analysis indicates the presence of orbital overlap between the two groups, although it does not indicate a strong electronic preference for either the *E*- or *Z*-configuration of the imine double bond.

Experimental Section

General Methods. All manipulations were carried out under dry nitrogen using standard Schlenk-line and cannula techniques, or in a conventional nitrogen-filled glovebox. Solvents were dried over appropriate drying agent and degassed prior to use. NMR spectra were recorded using a Bruker Avance DPX 300 MHz spectrometer at 300.1 (^{1}H), 75.4 (^{13}C{^{1}H}), 121.4 (^{31}P{^{1}H}) MHz and a Bruker AMX 500 MHz spectrometer at 500.1 (^{1}H), 125.7 (^{13}C{^{1}H}), 202.4 (^{31}P{^{1}H}) and 95.3 (^{77}Se{^{1}H}) MHz, from samples at 298 K in [$^2H_6$]-benzene, unless otherwise stated. Coupling constants are quoted in Hz. Proton and carbon chemical shifts were referenced internally to residual solvent resonances, phosphorus and selenium were referenced externally to H_3PO_4 (aq) and $SeMe_2$ ($CDCl_3$), respectively. Elemental analyses were performed by S. Boyer at the London Metropolitan University.

The reagents Ph_2PH (Fluka), Cy_2PH (Strem), ^{i}PrN═C═N^{i}Pr (Aldrich), CyN═C═NCy (Aldrich), S (Aldrich), Se (gray, Aldrich), BH_3·THF (1.0 M solution in THF, Aldrich), and ^{n}BuLi (2.5 M in hexanes, Acros) were purchased from commercial sources and used as received. $[HNEt_3][Cl]$ (Aldrich) was recrystallized from anhydrous chloroform, dried by heating in vacuo for 1 h, and stored under N_2. The phosphaguanidines $Ph_2PC\{N^iPr\}\{NH^iPr\}$ {**1a**} and $Ph_2PC\{NCy\}\{NHCy\}$ {**1b**} were made according to literature procedures.[9]

$Cy_2PC\{N^iPr\}\{NH^iPr\}$ (2a). From a solution of a 2.0 M ^{n}BuLi in hexanes (5.6 mmol) 2.80 mL was added dropwise to a solution of Cy_2PH (1.00 g, 5.0 mmol) in THF (∼20 mL) at 0 °C. The resultant pale-yellow solution was stirred for 20 min prior to the addition of ^{i}PrN═C═N^{i}Pr (0.90 mL, 5.5 mmol) to afford a clear colorless solution. After stirring at ambient temperature for 4 h, the reaction mixture was added to a slurry of $[HNEt_3][Cl]$ (0.80 g, 5.5 mmol) in THF (∼10 mL), affording a clear colorless solution. Removal of volatiles after 16 h yielded a crude white solid, from which the product was extracted by filtration, using hexane as the solvent. Concentration and storage of the resultant solution at −30 °C afforded analytically pure **2a** as colorless needles. Yield 1.23 g (75%).

Anal. Calcd for $C_{19}H_{37}N_2P$ (*324.48*): C, 70.33; H, 11.49; N, 8.63. Found: C, 70.32; H, 11.41; N, 8.79. ^{1}H NMR (500 MHz): *Major isomer* (E_{syn}) δ 4.71 (m, 1H, C*H*Me$_2$), 4.41 (sept, $^3J_{HH}$ = 6.5, 1H, C*H*Me$_2$), 3.59 (d, $^3J_{HH}$ = 6.8, 1H, N*H*), 1.99 (m, 2H, α-C*H* Cy), 1.79−0.96 (m, 20H, Cy), 1.37 (d, $^3J_{HH}$ = 6.2, 6H, CH*Me*$_2$), 1.09 (d, $^3J_{HH}$ = 6.4, 6H, CH*Me*$_2$). *Minor isomer* (Z_{anti}) δ 4.41 (sept, $^3J_{HH}$ = 6.5, 1H, C*H*Me$_2$), 3.91 (dd, J = 14.5, 1H, N*H*), 3.36 (sept, $^3J_{HH}$ = 6.5, 1H, C*H*Me$_2$), 2.22 (m, 2H, α-C*H* Cy), 1.79−0.96 (m, 20H + 6H, Cy, plus CH*Me*$_2$), 0.94 (d, $^3J_{HH}$ = 6.3, 6H, CH*Me*$_2$). ^{13}C{^{1}H} NMR (125 MHz): *Major isomer* (E_{syn}) δ 154.0 (d, $^1J_{CP}$ = 38, P*C*N$_2$), 51.5 (d, $^3J_{CP}$ = 39, ═N*C*H), 42.0 (−NH*C*H), 34.5 (d, $^1J_{CP}$ = 18, α-*C*H Cy), 31.5 (d, J_{CP} = 18, Cy), 30.3 (d, J_{CP} = 9, Cy), 27.3 (d, J_{CP} = 10, Cy), 27.2 (d, J_{CP} = 14, Cy), 26.6 (Cy), 25.8 (CH*Me*$_2$), 22.9 (CH*Me*$_2$). *Minor isomer* (Z_{anti}) δ 157.1 (d, $^1J_{CP}$ = 7, P*C*N$_2$), 51.8 (d, $^3J_{CP}$ = 31, ═N*C*H),

(34) Garner, C. D.; Howlader, N. C.; Mabbs, F. E.; Boorman, P. M.; King, T. J. *J. Chem. Soc., Dalton Trans.* **1978**, 1350; Burford, N.; Royan, B. W.; Spence, R. E. v. H.; Rogers, R. D. *J. Chem. Soc., Dalton Trans.* **1990**, 2111; Fornies, J.; Navarro, R.; Sicilia, V.; Tomas, M. *Inorg. Chim. Acta* **1990**, *168*, 201; Stumpf, K.; Blachnik, R.; Roth, G.; Kastner, G. *Z. Kristallogr. - New Cryst. Struct.* **2000**, *215*, 589; Hussain, M. S.; Isab, A. A.; Saeed, A.; Al-Arfaj, A. R. *Z. Kristallogr. - New Cryst. Struct.* **2001**, *216*, 629; Chutia, P.; Kumari, N.; Sharma, M.; Woolins, J. D.; Slawin, A. M. Z.; Dutta, D. K. *Polyhedron* **2004**, *23*, 1657; Cook, J. B.; Nicholson, B. K.; Smith, D. W. *J. Organomet. Chem.* **2004**, *689*, 860.

46.6 (−NH*C*H), 45.3 (d, $^1J_{CP}$ = 23, α-*C*H Cy), 34.0 (d, J_{CP} = 12, Cy), 29.9 (d, J_{CP} = 9, Cy), 27.7 (d, J_{CP} = 9, Cy), 27.5 (d, J_{CP} = 7, Cy), 27.1 (Cy), 24.6 (CH*Me*$_2$), 23.9 (CH*Me*$_2$). ^{31}P{^{1}H} NMR: *Major isomer* (E_{syn}) δ −21.2. *Minor isomer* (Z_{anti}) δ −4.8.

Cy$_2$PC{NCy}{NHCy} (2b). This compound was prepared in a manner analogous to that described for **2a**, using the following quantities: Cy$_2$PH (1.00 g, 5.0 mmol), ^{n}BuLi (2.80 mL of a 2.0 M solution in hexanes, 5.6 mmol), CyN═C═NCy (1.20 g, 5.5 mmol), and [HNEt$_3$][Cl] (0.80 g, 5.5 mmol). The compound was isolated from hexane at −30 °C as pale-yellow needles. Yield 1.65 g (81%).

Anal. Calcd for $C_{25}H_{45}N_2P$ (*404.61*): C, 74.21; H, 11.21; N, 6.92. Found: C, 74.18; H, 11.12; N, 6.93. ^{1}H NMR: *Major isomer* (E_{syn}) δ 4.37 (m, 1H, α-C*H* N−Cy), 4.19 (m, 1H, −C*H*, N−Cy), 3.74 (d, $^3J_{HH}$ = 6.9, 1H, N*H*), 2.07−0.84 (m, 42H, Cy). ^{13}C{^{1}H} NMR: *Major isomer* (E_{syn}) δ 153.9 (d, $^1J_{CP}$ = 38, P*C*N$_2$), 59.7 (d, $^3J_{CP}$ = 37, ═N*C*H), 48.8 (−NH*C*H), 36.3 (N−Cy), 34.8 (d, $^1J_{CP}$ = 17, α-*C*H P−Cy), 33.5 (N−Cy), 31.5 (d, J_{PC} = 18, P−Cy), 30.4 (d, J_{CP} = 9, P−Cy), 27.4 (d, J_{CP} = 12, P−Cy), 27.3 (d, J_{CP} = 16, P−Cy), 26.7 (N−Cy), 26.6 (Cy), 26.5 (Cy), 25.4 (Cy), 25.3 (Cy). (Only ^{1}H and ^{31}C{^{1}H} NMR data corresponding to the major isomer (E_{syn}) can be accurately reported due to the low intensity of the resonances from the minor species (Z_{anti}) and coincident chemical shifts of many signals.) ^{31}P{^{1}H} NMR: *Major isomer* (E_{syn}) δ −21.1. *Minor isomer* (Z_{anti}) δ −4.1.

Ph$_2$P(S)C{N^{i}Pr}{NH^{i}Pr} (3a). A suspension of elemental sulfur (32 mg, 1.00 mmol) in toluene (∼20 mL) was added dropwise at room temperature to a solution of Ph$_2$PC{N^{i}Pr}{NH^{i}Pr} (0.31 g, 1.0 mmol) in toluene (∼10 mL), and the resultant solution was stirred for 8 h. Removal of the volatiles in vacuo afforded an off-white oil, which was dissolved in heptane and filtered to remove residual chalcogen. Purification was achieved by slowly cooling the hot (∼75 °C) heptane solution to ambient temperature. Yield (colorless crystals) 0.25 g (72%).

Anal. Calcd for $C_{19}H_{25}N_2PS$ (*344.46*): C, 66.25; H, 7.31; N, 8.13. Found: C, 66.00; H, 7.22; N, 7.80. ^{1}H NMR: *Major isomer* (E_{syn}) δ 7.93 (m, 4H, *o*-C$_6$*H*$_5$), 6.98 (m, 6H, *m*- and *p*-C$_6$*H*$_5$), 5.20 (m, 1H, N*H*), 4.21 (m, 2H, −NHC*H* and ═NC*H*), 1.02 (d, $^3J_{HH}$ = 6.0, 6H, CH*Me*$_2$), 1.00 (d, $^3J_{HH}$ = 6.5, 6H, CH*Me*$_2$). *Minor isomer* (Z_{syn}) δ 8.28 (m, 4H, *o*-C$_6$*H*$_5$), 7.04 (m, 6H, *m*- and *p*-C$_6$*H*$_5$), 6.77 (m, 1H, N*H*), 3.82 (sept, $^3J_{HH}$ = 5.9, 1H, −NHC*H*), 3.60 (m, 1H, ═NC*H*), 1.07 (d, $^3J_{HH}$ = 6.1, 6H, CH*Me*$_2$), 0.82 (d, $^3J_{HH}$ = 6.3, 6H, CH*Me*$_2$). ^{13}C{^{1}H} NMR: δ 147.5 (d, $^1J_{CP}$ = 131, P*C*N$_2$), 144.2 (d, $^1J_{CP}$ = 54, P*C*N$_2$), 133.0 (d, J_{CP} = 76, *C*$_6$H$_5$), 132.9 (d, J_{CP} = 10, *C*$_6$H$_5$), 132.2 (d, J_{CP} = 11, *C*$_6$H$_5$), 131.5 (d, J_{CP} = 43, *C*$_6$H$_5$), 131.4 (d, J_{CP} = 43, *C*$_6$H$_5$), 128.8 (d, J_{CP} = 12, *C*$_6$H$_5$), 128.0 (d, J_{CP} = 12, *C*$_6$H$_5$), 50.7 (d, J_{CP} = 16, *C*HMe$_2$), 49.3 (d, J_{CP} = 21, *C*HMe$_2$), 46.7 (d, J_{CP} = 9, *C*HMe$_2$), 43.7 (d, J_{CP} = 5, *C*HMe$_2$), 24.4 (CH*Me*$_2$), 24.3 (CH*Me*$_2$), 23.8 (CH*Me*$_2$), 22.1 (CH*Me*$_2$). (^{13}C{^{1}H} NMR data have not been individually assigned for each isomer and are reported together.) ^{31}P{^{1}H} NMR: *Major isomer* (Z_{syn}) δ 33.6. *Minor* isomer (E_{syn}) δ 38.2.

Ph$_2$P(S)C{NCy}{NHCy} (3b). This compound was prepared in a manner analogous to that described for **3a**, using the following quantities: Ph$_2$PC{NCy}{NHCy} (0.47 g, 1.2 mmol) and elemental sulfur (40 mg, 1.20 mmol). The compound was crystallized from heptane as described for **3a**. Yield (colorless crystals) 0.48 g (95%).

Anal. Calcd for $C_{25}H_{33}N_2PS$ (*424.58*): C, 70.72 H, 7.83; N, 6.60. Found: C, 70.95; H, 7.91; N, 6.55. ^{1}H NMR: *Major isomer* (Z_{syn}) δ 7.99 (m, 4H, *o*-C$_6$*H*$_5$), 6.98 (m, 6H, *m*- and *p*-C$_6$*H*$_5$), 5.53 (m, 1H, N*H*), 4.09 (m, 1H, −NHC*H*), 3.88 (m, 1H, ═NCH), 1.95−0.90 (m, 20H, Cy). *Minor isomer* (E_{syn}) δ 8.33 (m, 4H, *o*-C$_6$*H*$_5$), 6.98 (m, 6H, *m*- and *p*-C$_6$*H*$_5$), 6.90 (m, 1H, N*H*), 3.65 (m, 1H, ═NC*H*), 3.44 (m, 1H, −NHC*H*), 1.95−0.90 (m, 20H, Cy). ^{13}C{^{1}H} NMR: δ 147.5 (d, J_{CP} = 132, P*C*N$_2$), 144.0 (d, J_{CP} = 52, P*C*N$_2$), 133.8 (d, J_{CP} = 70, *C*$_6$H$_5$), 133.2 (d, J_{CP} = 57, *C*$_6$H$_5$), 132.9 (d, J_{CP} = 10, *C*$_6$H$_5$), 132.2 (d, J_{CP} = 11, *C*$_6$H$_5$), 131.7 (d, J_{CP} = 3, *C*$_6$H$_5$), 131.2 (d, J_{CP} = 3, *C*$_6$H$_5$), 128.4 (d, J_{CP} = 12, *C*$_6$H$_5$), 127.7 (d, J_{CP} = 12, *C*$_6$H$_5$), 58.5 (d, $^3J_{CP}$ = 24, α-*C*H), 57.4 (d, $^3J_{CP}$ = 8, α-*C*H), 53.8 (d, $^3J_{CP}$ = 22, α-*C*H), 50.2, 34.8, 34.5, 34.2, 32.1, 26.3, 26.2, 26.1, 25.5, 24.8, 24.6 (Cy). (^{13}C{^{1}H} NMR data have not been individually assigned for each isomer and are reported together.) ^{31}P{^{1}H} NMR: *Major isomer* (Z_{syn}) δ 34.0. *Minor isomer* (E_{syn}) δ 38.6.

Ph$_2$P(Se)C{N^{i}Pr}{NH^{i}Pr} (4a). This compound was prepared in a manner analogous to that described for **3a**, using the following quantities: Ph$_2$PC{N^{i}Pr}{NH^{i}Pr} (0.31 g, 1.0 mmol) and gray selenium (80 mg, 1.00 mmol). The compound was crystallized from heptane as described for **3a**. Yield (colorless crystals) 0.29 g (74%). Despite repeated attempts, accurate elemental analysis could not be obtained for this compound, with results consistent with the presence of residual selenium.

^{1}H NMR: *Major isomer* (E_{syn}) δ 7.93 (m, 4H, *o*-C$_6$*H*$_5$), 6.97 (m, 6H, *m*- and *p*-C$_6$*H*$_5$), 5.29 (m, 1H, N*H*), 4.201 (m, 2H, −NHC*H* and ═NC*H*), 1.00 (d, $^3J_{HH}$ = 6.1, 12 H, CH*Me*$_2$). *Minor isomer* (Z_{syn}) δ 8.21 (m, 4H, *o*-C$_6$*H*$_5$), 7.02 (m, 6H, *m*- and *p*-C$_6$*H*$_5$), 6.87 (m, 1H, N*H*), 3.81 (sept, $^3J_{HH}$ = 6.1, 1H, −NHC*H*), 3.60 (m, 1H, ═NC*H*), 1.04 (d, $^3J_{HH}$ = 6.1, 6H, CH*Me*$_2$), 0.85 (d, $^3J_{HH}$ = 6.2, 6H, CH*Me*$_2$). ^{13}C{^{1}H} NMR: δ 145.9 (d, $^1J_{CP}$ = 122, P*C*N$_2$), 141.6 (d, $^1J_{CP}$ = 42, P*C*N$_2$), 133.3 (d, J_{CP} = 10, *C*$_6$H$_5$), 132.6 (d, J_{CP} = 11, *C*$_6$H$_5$), 132.6 (d, J_{CP} = 76, *C*$_6$H$_5$), 132.7 (d, J_{CP} = 79, *C*$_6$H$_5$), 131.5 (d, J_{CP} = 39, *C*$_6$H$_5$), 132.4 (d, J_{CP} = 39, *C*$_6$H$_5$), 128.8 (d, J_{CP} = 12, *C*$_6$H$_5$), 128.0 (d, J_{CP} = 12, *C*$_6$H$_5$), 50.7 (d, J_{CP} = 16, *C*HMe$_2$), 49.4 (d, J_{CP} = 21, *C*HMe$_2$), 46.8 (d, J_{CP} = 9, *C*HMe$_2$), 43.9 (d, J_{CP} = 5, *C*HMe$_2$), 24.3 (CH*Me*$_2$), 24.2 (CH*Me*$_2$), 23.7 (CH*Me*$_2$), 22.0 (CH*Me*$_2$). (^{13}C{^{1}H} NMR data have not been individually assigned for each isomer and are reported together.) ^{31}P{^{1}H} NMR: *Major isomer* (E_{syn}) δ 23.2 ($^1J_{PSe}$ = −755). *Minor isomer* (Z_{syn}) δ 35.2 ($^1J_{PSe}$ = −721). ^{77}Se{^{1}H} NMR ([^{2}H]$_8$-toluene): *Major isomer* (E_{syn}) δ −222 ($^1J_{SeP}$ = −755). *Minor isomer* (Z_{syn}) δ −304 ($^1J_{SeP}$ = −721).

Ph$_2$P(Se)C{NCy}{NHCy} (4b). This compound was prepared in a manner analogous to that described for **3a**, using the following quantities: Ph$_2$PC{NCy}{NHCy} (0.50 g, 1.3 mmol) and gray selenium (100 mg, 1.27 mmol). The compound was crystallized from heptane as described for **3a**. Yield (colorless crystals) 0.39 g (65%).

Anal. Calcd for $C_{25}H_{33}N_2PSe$ (*471.48*): C, 63.69; H, 7.05; N, 5.94. Found: C, 63.61; H, 7.22; N, 5.74. ^{1}H NMR: δ *Major isomer* (E_{syn}) δ 7.98 (m, 4H, *o*-C$_6$*H*$_5$), 7.02 (m, 6H, *m*- and *p*-C$_6$*H*$_5$), 5.59 (m, 1H, N*H*), 4.06 (m, 1H, −NHC*H*), 3.85 (m, 1H, ═NC*H*), 1.94−0.88 (m, 20H, Cy). *Minor isomer* (Z_{syn}) δ 8.26 (m, 4H, *o*-C$_6$*H*$_5$), 7.02 (m, 6H, *m*- and *p*-C$_6$*H*$_5$), 6.96 (m, 1H, N*H*), 3.65 (m, 1H, ═NC*H*), 3.45 (m, 1H, −NHC*H*), 1.94−0.88 (m, 20H, Cy). ^{13}C{^{1}H} NMR ([^{2}H]$_8$-toluene): δ 145.6 (d, J_{CP} = 123, P*C*N$_2$), 141.3 (d, J_{CP} = 43, P*C*N$_2$), 132.7 (d, J_{CP} = 77, *C*$_6$H$_5$), 132.5 (d, J_{CP} = 68, *C*$_6$H$_5$), 133.2 (d, J_{CP} = 10, *C*$_6$H$_5$), 132.6 (d, J_{CP} = 11, *C*$_6$H$_5$), 131.6 (d, J_{CP} = 3, *C*$_6$H$_5$), 131.0 (d, J_{CP} = 3, *C*$_6$H$_5$), 128.7 (d, J_{CP} = 12, *C*$_6$H$_5$), 127.8 (d, J_{CP} = 12, *C*$_6$H$_5$), 58.4 (d, $^3J_{CP}$ = 15, α-*C*H), 57.4 (d, $^3J_{CP}$ = 18, α-*C*H), 53.8 (d, $^3J_{CP}$ = 10, α-*C*H), 50.3 (d, $^3J_{CP}$ = 6, α-*C*H), 34.4, 34.0, 32.1, 26.2, 26.1, 25.5, 24.4 (Cy). (^{13}C{^{1}H} NMR data for both isomer are indistinguishable from one another and are reported together.) ^{31}P{^{1}H} NMR: *Major isomer* (E_{syn}) δ 23.9 ($^1J_{PSe}$ = −753). *Minor isomer* (Z_{syn}) δ 35.5 ($^1J_{PSe}$ = −721). ^{77}Se{^{1}H} NMR ([^{2}H]$_8$-toluene): *Major isomer* (E_{syn}) δ −224 ($^1J_{SeP}$ = −753). *Minor isomer* (Z_{syn}) δ −311 ($^1J_{SeP}$ = −721, $J_{Se\cdots H}$ = 6).

Cy$_2$P(S)C{N^{i}Pr}{NH^{i}Pr} (5a). This compound was prepared in a manner analogous to that described for **3a**, using the following quantities: Cy$_2$PC{N^{i}Pr}{NH^{i}Pr} (0.10 g, 0.3 mmol) and excess elemental sulfur (20 mg, 0.62 mmol). The compound was crystallized from heptane as described for **3a**. Yield (colorless crystals) 0.067 g (61%).

Anal. Calcd for $C_{19}H_{37}N_2PS$ (*356.54*): C, 64.00; H, 10.46; N, 7.86. Found: C, 63.91; H,10.35; N, 7.84. ^{1}H NMR: *Major isomer* (Z_{syn}) δ 6.64 (dd br, J = 7.3, 1H, N*H*), 3.85 (sept, $^3J_{HH}$ = 6.0, 1H, C*H*Me$_2$), 3.60 (m, 1H, C*H*Me$_2$), 2.32−1.52 (m, 22H, Cy), 1.16 (d, $^3J_{HH}$ = 6.1, 6H, CH*Me*$_2$), 0.92 (d, $^3J_{HH}$ = 6.3, 6H, CH*Me*$_2$). ^{13}C{^{1}H} NMR: *Major isomer* (Z_{syn}) δ 145.2 (d, $^1J_{CP}$ = 114, P*C*N$_2$), 48.6 (d, $^3J_{CP}$ = 20, ═NCH), 46.6 (d, $^3J_{CP}$ = 8, −NH*C*H), 38.2 (d, $^1J_{CP}$ = 50, α-*C*H Cy),

26.9, 26.7, 26.6, 26.5, 26.4, 26.3, 26.1 (nonassigned resonances corresponding to an overlapping series of doublets (J_{CP}) from the methylene groups of the cyclohexyl substituents) 24.9 (CH*Me*$_2$), 24.0 (CH*Me*$_2$). (Only the ^{1}H and ^{13}C{^{1}H} NMR data for the major (Z_{syn}) component can be reported with confidence, due to the low intensity of the resonances corresponding to the minor (E_{syn}) species.) ^{31}P{^{1}H} NMR: *Major isomer* (Z_{syn}) δ 63.3. *Minor isomer* (E_{syn}) δ 67.4.

Cy$_2$P(S)C{NCy}{NHCy} (5b). This compound was prepared in a manner analogous to that described for **3a**, using the following quantities: Cy$_2$PC{NCy}{NHCy} (0.10 g, 0.2 mmol) and elemental sulfur (20 mg, 0.50 mmol). The compound was crystallized from heptane as described for **3a**. Yield (colorless crystals) 0.063 g, (58%). Anal. Calcd for $C_{25}H_{45}N_2PS$ (*436.68*): C, 68.76; H, 10.39; N, 6.42. Found: C, 68.62; H, 10.26; N, 6.30. ^{1}H NMR: *Major isomer* (Z_{syn}) δ 6.83 (dd br, J = 7.4, 1H, N*H*), 3.63 (m, 1H, α-C*H*, N−Cy), 3.42 (m, 1H, α-C*H*, N−Cy), 2.41−1.07 (m, 42H, Cy). ^{13}C{^{1}H} NMR: *Major isomer* (Z_{syn}) δ 145.0 (d, $^1J_{CP}$ = 114, P*C*N$_2$), 57.1 (d, $^3J_{CP}$ = 19, =N*C*H), 53.8 (d, $^3J_{CP}$ = 8, −NH*C*H), 38.3 (d, $^1J_{CP}$ = 50, α-*C*H, Cy), 35.3, 34.5, 27.2, 27.0, 26.8, 26.6, 26.5 (×2), 26.4, 26.2, 25.6, 25.0, 24.6 (nonassigned resonances corresponding to an overlapping series of doublets (J_{CP}) from the methylene groups of the cyclohexyl substituents). (Only the ^{1}H and ^{13}C{^{1}H} NMR data for the major (Z_{syn}) component can be reported with confidence, due to the low intensity of the resonances corresponding to the minor (E_{syn}) species.) ^{31}P{^{1}H} NMR: *Major isomer* (Z_{syn}) δ 63.7. *Minor isomer* (E_{syn}) δ 67.0.

Cy$_2$P(Se)C{N^{i}Pr}{NH^{i}Pr} (6a). This compound was prepared in a manner analogous to that described for **3a**, using the following quantities: Cy$_2$PC{N^{i}Pr}{NH^{i}Pr} (0.10 g, 0.3 mmol) and elemental selenium (50 mg, 0.63 mmol). The compound was crystallized from heptane as described for **3a**. Yield (colorless crystals) 0.084 g, (67%).

Despite repeated attempts, accurate elemental analysis could not be obtained for **6a**. ^{1}H NMR: *Major isomer* (Z_{syn}) δ 6.72 (dd br, J = 7.0, 1H, N*H*), 3.83 (sept, $^3J_{HH}$ = 6.1, 1H, C*H*Me$_2$), 3.60 (m, 1H, C*H*Me$_2$), 2.40−1.51 (m, 22H, Cy), 1.15 (d, $^3J_{HH}$ = 6.1, 6H, CH*Me*$_2$), 0.93 (d, $^3J_{HH}$ = 6.3, 6H, CH*Me*$_2$). ^{13}C{^{1}H} NMR: *Major isomer* (Z_{syn}) δ 145.2 (d, $^1J_{CP}$ = 114, P*C*N$_2$), 48.7 (d, $^3J_{CP}$ = 19, =N*C*H), 46.8 (d, $^3J_{CP}$ = 9, −NH*C*H), 38.1 (d, $^1J_{CP}$ = 43, α-*C*H Cy), 26.8 (×2), 26.6, 26.6, 26.4, 26.4, 26.3, 26.0 (nonassigned resonances corresponding to an overlapping series of doublets (J_{CP}) from the methylene groups of the cyclohexyl substituents), 24.8 (CH*Me*$_2$), 23.9 (CH*Me*$_2$). (Only the ^{1}H and ^{13}C{^{1}H} NMR data for the major (Z_{syn}) component can be reported with confidence, due to the low intensity of the resonances corresponding to the minor (E_{syn}) species.) ^{31}P{^{1}H} NMR: *Major isomer* (Z_{syn}) δ 62.4 ($^1J_{PSe}$ = −692). *Minor isomer* (E_{syn}) δ 67.0 (coupling to selenium not recorded due to low intensity of the signal).

Cy$_2$P(Se)C{NCy}{NHCy} (6b). This compound was prepared in a manner analogous to that described for **3a**, using the following quantities: Cy$_2$PC{NCy}{NHCy} (0.10 g, 0.2 mmol) and elemental selenium (40 mg, 0.50 mmol). The compound was crystallized from heptane as described for **3a**. Yield (colorless crystals) 0.077 g, (64%).

Anal. Calcd for $C_{25}H_{45}N_2PSe$ (*483.57*): C, 62.09; H, 9.38; N, 5.79. Found: C, 62.09; H, 9.25; N, 5.79. ^{1}H NMR: *Major isomer* (Z_{syn}) δ 6.90 (dd br, J = 7.2, 1H, N*H*), 3.63 (m, 1H, α-C*H* N−Cy), 3.45 (m, 1H, α-C*H* N−Cy), 2.46−0.94 (m, 42H, Cy). ^{13}C{^{1}H} NMR (125 MHz): *Major isomer* (Z_{syn}) δ 143.2 (d, $^1J_{CP}$ = 107, P*C*N$_2$), 57.2 (d, $^3J_{CP}$ = 18, =N*C*H), 53.9 (d, $^3J_{CP}$ = 8, −NH*C*H), 38.2 (d, $^1J_{CP}$ = 42, α-*C*H Cy), 35.3, 34.4, 26.9, 26.8, 26.7, 26.6, 26.5, 26.3, 25.6, 24.9, 24.5 (nonassigned resonances corresponding to an overlapping series of doublets (J_{CP}) from the methylene groups of the cyclohexyl substituents). ^{31}P{^{1}H} NMR: *Major isomer* (Z_{syn}) δ 62.7 ($^1J_{PSe}$ = −688). *Minor isomer* (E_{syn}) δ 66.4 (coupling to selenium not recorded due to low intensity of the signal). ^{77}Se{^{1}H} NMR: *Major isomer* (Z_{syn}) δ −467 ($^1J_{SeP}$ = −690, $J_{Se\cdots H}$ = 6). (Only the ^{1}H, ^{13}C{^{1}H}, and ^{77}Se-{^{1}H} NMR data for the major (Z_{syn}) component can be reported with confidence, due to the low intensity of the resonances corresponding to the minor (E_{syn}) species.)

Ph$_2$P(BH$_3$)C{NCy}{NHCy} (7). A solution of BH$_3$·THF (0.25 mL of a 1.0 M solution in THF, 0.3 mmol) was added dropwise via syringe to a solution of Ph$_2$PC{NCy}{NHCy} (0.10 g, 0.3 mmol) in THF at room temperature. The resultant solution was stirred for 12 h, after which time the volatiles were removed under reduced pressure, affording a crude white oil. Crystallization from hexane at −30 °C afforded analytically pure **7**. Yield (colorless crystals) 0.022 g (22%).

Anal. Calcd for $C_{25}H_{36}BN_2P$ (*406.35*): C, 73.89; H, 8.93; N, 6.89. Found: C, 73.73; H, 8.64; N, 6.61. IR (Nujol mull, CsI, cm^{-1}): 3424m υ(N−H), 2395br υ(B−H), 1600 υ(C=N), 565 υ(P−B). Compound **7** was unstable in solution with respect to loss of borane, precluding the acquisition of reliable NMR data.

Details of the Crystallographic Study. Details of the crystal data, intensity collection, and refinement for complexes **2a**, {**3b**}, and {**4b**} are collected in Table 1 and for **5a**, **6a**, **6b**, and **7** in Table 2. Crystals were covered in an inert oil, and suitable single crystals were selected under a microscope and mounted on a Kappa CCD diffractometer. The structures were refined with SHELXL-97.[35] In all cases, the H-atom on the amine nitrogen was refined with other H-atoms in riding mode; the hydrogen atoms on boron in Ph$_2$P(BH$_3$)C{NCy}{NHCy} (**7**) were refined.

Details of the Computational Study. All calculations were performed using the Gaussian 03 suite of programs.[17] The model compounds that were examined were constructed using the Cartesian coordinates taken from the relevant X-ray structures. To simplify the calculations and limit the steric influence of the nitrogen substituents, the isopropyl and cyclohexyl groups were replaced with methyl groups using the GaussView suite of programs. To examine the relative energies of the α- and β-conformations, the amidine group was rotated about the P−C bond while the rest of the molecule was fixed. In all instances, full optimization and frequency calculations were performed using the B3LYP density functional theory and the 6-31G(d) basis set. Natural bond orbital (NBO) analyses[36] were calculated on optimized geometries.

Acknowledgment. We thank the University of Sussex for financial support and Drs. M. S. Hill and J. R. Fulton for helpful discussion during the preparation of this manuscript.

Supporting Information Available: A complete citation list for ref 17. This material is available free of charge via the Internet at http://pubs.acs.org.

JA064212T

(35) Sheldrick, G. M. *SHELXL-97*, Program for the Refinement of Crystal Structures; Göttingen, 1997.
(36) Foster, J. P.; Weinhold, F. *J. Am. Chem. Soc.* **1980**, *102*, 7211.